ISSN 0869-5911, Petrology, 2023, Vol. 31, No. 5, pp. 492–518. © Pleiades Publishing, Ltd., 2023.
Russian Text © The Author(s), 2023, published in Petrologiya, 2023, Vol. 31, No. 5, pp. 482–509.

Lower Talnakh Type Intrusions of the Norilsk Ore Region

S. F. Sluzhenikin[a], *, K. N. Malitch[b], M. A. Yudovskaya[a, c], D. M. Turovtsev[a, †], T. N. Antsiferova[a], S. K. Mikhalev[d], I. Yu. Badanina[b], and N. G. Soloshenko[b]

[a] *Institute of Geology of Ore Deposits, Petrography, Mineralogy and Geochemistry, Russian Academy of Sciences, Moscow, Russia*

[b] *Zavaritskii Institute of Geology and Geochemistry, Ural Branch, Russian Academy of Sciences, Yekaterinburg, Russia*

[c] *CIMERA, School of Geosciences, University of Witwatersrand, Wits 2050, South Africa*

[d] *LLC "Norilskgeology," Norilsk, Russia*

**e-mail: sluzhenikinsf@yandex.ru*

Received October 26, 2022; revised February 3, 2023; accepted February 15, 2023

Abstract—Troctolites, olivine and picrite gabbrodolerites account for up to 75% of the Lower Talnakh type intrusions in areas of their elevated thickness, whereas reduced sections consist of olivine-free and olivine-bearing gabbrodolerites. The high-Mg cumulates show no clear differentiation, although the contents of TiO_2 and alkalis increase towards the upper inner contacts. The transitions between the rock types are gradational, and the compositions of low-Ni olivine in different rocks ($Fo_{70–83}$, 0.01–0.2 wt % NiO) overlap significantly. Clinopyroxene ($Fs_{7–13}$, Mg# 68–89) is characterized by the lowest both contents and variation ranges of Cr_2O_3 (0.01–0.5 wt %) and TiO_2 (0.05–1.0 wt %) among all types of the intrusions of the Norilsk complex, which is consistent with the Cr-depleted (0.002–0.051 wt % Cr_2O_3) bulk rock compositions. Later orthopyroxene ($Fs_{15–30}$) is crystallized by the reaction of the residual melt with early olivine. Plagioclase forms porphyritic phenocrysts and their intergrowths along with ophitic laths, and also predominates in schlierens and fragments of leucocratic rocks in taxitic and picritic gabbrodolerites with a weakly sorted layered texture. In olivine-rich rocks, sulfides are represented by the association of troilite ± hexagonal pyrrhotite + Fe- and Co-rich pentlandite + Fe-enriched chalcopyrite (±putoranite, talnakhite) ± cubanite. The upper and lower parts of the intrusions contain association of hexagonal pyrrhotite + chalcopyrite + pentlandite, while monoclinic pyrrhotite + chalcopyrite + Ni-enriched pentlandite are formed in the inner- and outer contacts. The concentration of base (0.077–0.21 wt % Ni, 0.05–0.38 wt % Cu) and platinum metals (0.03–0.26 to 0.40 ppm total PGE) in mineralized rocks is very low. Upon small amounts of sulfides and extremely low base and platinum metal tenors, the heterogeneous S isotopic composition of the Lower Talnakh type sulfides ($\delta^{34}S$ mainly 3.8–8.6‰, but reaches up to 11.8‰) most likely reflects the attainment of repeated sulfide saturation during the assimilation of sulfate S by magma that has previously experienced the loss of chalcophile metals into a coexisting sulfide liquid at a depth. The Sr-Nd isotopic compositions of the Lower Talnakh intrusions (Sr_i—from 0.7073 to 0.7087 and $\varepsilon_{Nd}(T)$ from –1.8 to –5.9 calculated for 250 Ma) show the predominant contribution of the Proterozoic material, in contrast to the ore-bearing intrusions, which Sr-Nd isotope compositions indicate the contamination with Paleozoic upper crustal sedimentary rocks.

Keywords: magmatic sulfides, mafic-ultramafic intrusions, Lower Talnakh type, Norilsk region, Nd-Sr isotope systematics, S-Cu isotope systematics, contamination, trap magmatism

DOI: 10.1134/S0869591123050065

INTRODUCTION

The Lower Talnakh type intrusions belong to the Norilsk complex of the Norilsk region along with the Kruglogorka, Zubov, and Norilsk type intrusions (Lyul'ko et al., 1975; Rad'ko, 2016). The latter type includes the economic-grade Talnakh, Kharaelakh, Norilsk-1, Norilsk-2, and Chernogorka and potentially ore-bearing Imangda, Mantur, Mikchangda, and Talmi massifs (Fig. 1). The high-grade disseminated mineralization was also established in the Zubov type intrusions (Pyasino–Vologochan) and in separate areas of the Kruglogorka type sills (Sluzhenikin et al., 2018, 2020). Compared to the intrusions of the other types of the Norilsk complex, the Lower Talnakh type is sulfide-bearing while with extremely low Ni

† Deceased.

and Cr contents and ascribed to a group of melanocratic intrusions with high percentage of olivine-rich rocks (Dyuzhikov et al., 1988; Turovtsev, 2002). The Lower Talnakh type intrusions together with the ore-bearing chonoliths are components of the multilevel magmatic plumbing systems, which complex and staged structure reflects the favorable settings for emplacement. At the known ore fields, the lateral extension of the Lower Talnakh intrusions is much wider than the area of the associated ore-bearing chonoliths and the former can be used as prospecting criterion for the search of ore-bearing chonoliths in the new fields. In this relation, their localization in the host sequence, relationships with other intrusions, their inner structure as a reflection of source and subsequent magmatic differentiation are of great importance both for understanding the magmatic evolution of the region and developing exploration strategy.

The geological structure, petrographic composition, and isotope-geochemical features of the Lower Talnakh intrusions were characterized to different extent (Dodin and Sadikov, 1967; Natorkhin et al., 1977; Zemskova, 1981; Dyuzhikov et al., 1988; Naldrett et al., 1992, 1995; Zen'ko and Czamanske, 1994; Czamanske et al., 1992; Hawkesworth et al., 1995; Arndt et al., 2003; Ryabov et al., 2000; Turovtsev, 2002; Ryabov et al., 2014; Krivolutskaya, 2014). In the earlier works, these intrusions were ascribed to the Morongo complex (Dodin and Sadikov, 1967; Komarov and Lyul'ko, 1967). According to Zemskova (1981), the Lower Talnakh type includes, in addition to the Lower Talnakh, Lower Norilsk intrusions and Klyukvenny intrusion in the Talmi cluster, also the Zub-Marksheider and Vologochan intrusions, which were later ascribed to the Zubov type intrusions (Turovtsev, 2002; Sluzhenikin et al., 2020; Sluzhenikin and Krivolutskaya, 2015), as well as the Mantur intrusion in the Imangda cluster. Lyul'ko et al. (1975) ascribed the Lower Talnakh intrusions to the Norilsk complex based on their spatial association with the ore-bearing intrusions. The Lower Talnakh intrusions were proposed later to represent a discrete intrusive complex on its own (Fedorenko, 2010; Paderin et al., 2016), given their specific chemical and isotope characteristics.

The Lower Talnakh intrusion is distinguished as the petrotype studied in most detail that made it possible to constrain the indicative isotope-geochemical characteristics of the Lower Talnakh type (Zen'ko and Czamanske, 1994; Hawkesworth et al., 1995; Arndt et al., 2003; *Izotopnaya geologiya* ..., 2017; Malitch et al., 2018). Data on the Lower Norilsk, Zelenaya Griva, and Klyukvenny intrusions are fewer and represented mainly in the exploration reports, while their sulfide mineralization received even less attention (Avgustinchik, 1981).

This paper provides systematic characteristics of the geological structure, petrographic and mineral composition of rocks, as well as sulfide mineralization of three Lower Talnakh type intrusions: the Lower Talnakh, Lower Norilsk, and Zelenaya Griva. The Sr and Nd isotope data, as well as S and Cu isotope systematics in rocks and minerals of these intrusions support the predominant deep-seated contamination of the Lower Talnakh magmas and subordinate role of a local contamination trend, which has been previously revealed for the ore-bearing intrusions (Arndt et al., 2003).

GEOLOGICAL AND STRUCTURAL POSITION OF THE LOWER TALNAKH TYPE INTRUSONS

The Lower Talnakh intrusion occurs in the Talnakh ore cluster as well as beyond its limits (Fig. 2). Its distribution is mainly controlled by the Norilsk–Kharaelakh and Fokina–Tangaralakh faults (Fig. 1).

The boundaries of the Lower Talnakh intrusion are not established continuously and complicated by numerous apophyses over the entire periphery. In the southwest, its boundary is outlined by its sub-exposures beneath the Quaternary deposits at the margin of the Kharaelakh depression (Fig. 2). In a plan view, the Lower Talnakh intrusion is subdivided into the Western, Central, and Eastern parts (branches) (Fig. 2). To the west of the Norilsk–Kharaelakh fault, the intrusion is hosted mainly in rocks of the Lower Devonian Razvedochninsk, Kureika, and Zubov formations (Figs. 2, 3) in a form of a bent band in plan. In the zone of the Axial (Daldykan) fault, the Western branch of the Lower Talnakh intrusion lies stratigraphically lower than the ore-bearing Kharaelakh intrusion and associated Kruglogorka type intrusion. In the fault zone, the thickness of the branch sharply increases from 35 to 130 m. This zone of elevated thicknesses outlines the ore-bearing Kharaelakh intrusion from the west.

The Central branch of the intrusion is confined to the Norilsk–Kharaelakh fault and controlled by a structure complicating the western limb of this fault. The thickness of the Lower Talnakh intrusion in this area reaches 412 m (drill hole KZ-108). This band of elevated thicknesses is characterized by the large amplitude in thickness variations from 40 to 400 m. The intrusion is complicated by bulges, flexures, pinches and splittings, and slightly rises in the stratigraphic sequence up to the boundary of the Kureika–

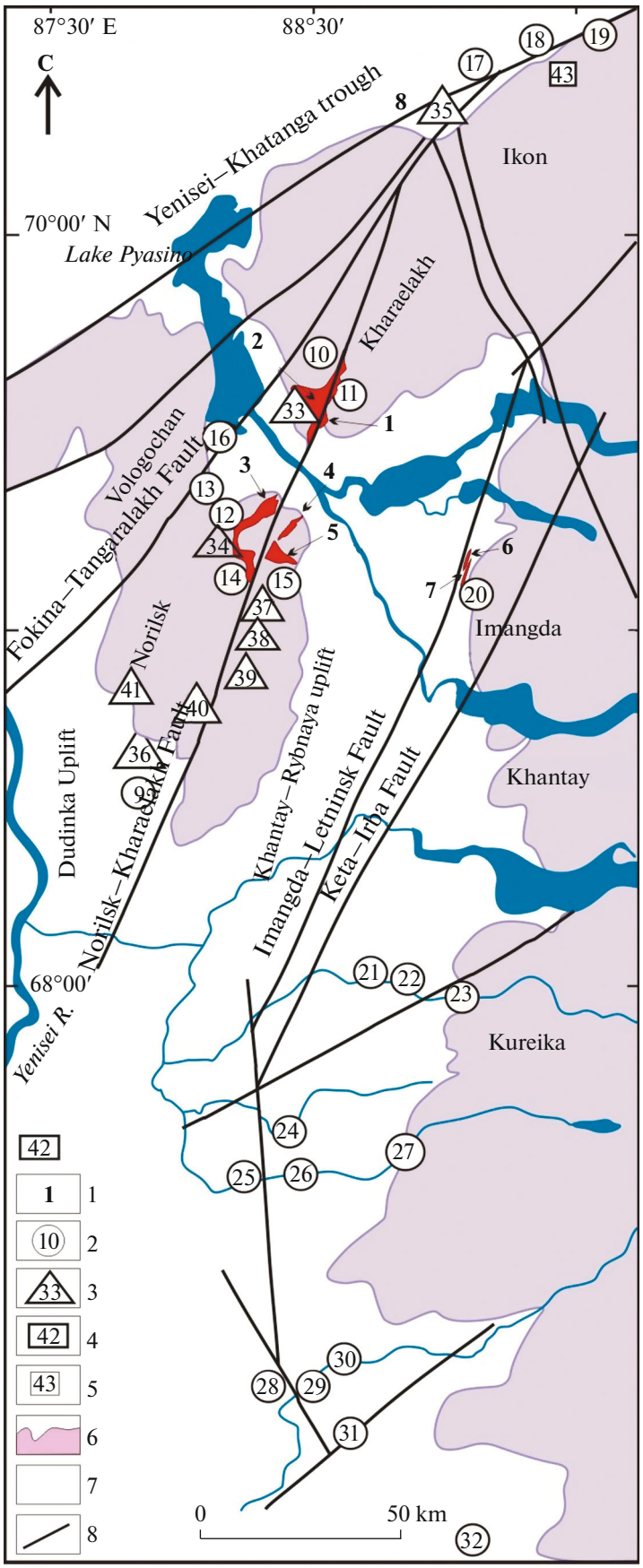
87°30′ E
88°30′
C
70°00′ N
68°00′
Yenisei–Khatanga trough
Lake Pyasino
Yenisei R.
Kharaelakh
Vologochan Fault
Fokina–Tangaralakh Fault
Norilsk
Norilsk–Kharaelakh Fault
Dudinka Uplift
Khantay–Rybnaya uplift
Imangda–Letninsk Fault
Keta–Irba Fault
Ikon
Imangda
Khantay
Kureika
0
50 km
1
2
3
4
5
6
7
8

Fig. 1. Distribution scheme of the differentiated ultramafic–mafic intrusions in the Norilsk region. (1–3) types of differentiated mafic-ultramafic intrusions: (1) *mesocratic type* (intrusions: (1) Talnakh, (2) Kharaelakh, (3) Norilsk-1, (4) Norilsk-2, (5) Chernogorka, (6) Imangda, (7) Mantur, (8) Talmi); (2) *leucocratic type* (intrusions: (9) Burkan, (10) Tangaralakh, (11) Gabbrovy, (12) Zubov, (13) Verkhneambarninsk, (14) Verkhnebystrinsk, (15) Kruglogorka, (16) Pyasino-Vologochan, (17) Ikon, (18) Yttakh, (19) Arylakh–Mastakhsalin, (20) Nakokhoz, (21) Verkhneiltyk, (22) Silurisk, (23) Kulyumbe, (24) Brussk, (25) Nizhnegorbiyachin, (26) Dzhaltul, (27) Verkhnegorbiyachin, (28) Nizhnii, (29) Svetlogorsk, (30) Vtorogo poroga Kureika R.; (31) Okunevoozersk, (32) Kolyui); (3) *melanocratic type* (intrusions: (33) Lower Talnakh, (34) Lower Norilsk, (35) Klyukvenny; (36) Zelenaya Griva, (37) Pikritovyi Ruchei, (38) Morongo, (39) Magnitny Ruchei, (40) Mt. Pikritov, (41) Nizhnefokinsk); (4) deposits of cupriferous sandstones ((42) Sukharikhinsk); (5) native copper occurrences ((43) Arylakh); (6) undivided Permian–Triassic volcanogenic formations; (7) undivided terrigenous–sedimentary formations; (8) faults.

Razvedochninsk formations (Fig. 4; Supplementary,[1] ESM_3.pdf).

The Eastern branch is localized in the eastern limb of the Norilsk–Kharaelakh fault and significantly overlapped in a plan view with the ore-bearing Talnakh intrusion. In the south, the intrusion is hosted by rocks of the Lower Devonian Kureika and Zubov formations. The trough-shaped bottom of the intrusion is plunging to the north, approaching and even intersecting the Talnakh intrusions in the northern areas, where the Lower Talnakh intrusion is emplaced into rocks of the C_2–P_3 Tunguska Group above the ore-bearing Talnakh intrusion (Fig. 5; ESM_4.pdf (Suppl.)).

The Lower Norilsk intrusion lies to the west of the Norilsk-1 intrusion, in the Daldykan (Fokina–Tangaralakh) fault zone (Fig. 6). The massif is split by the Daldykan fault zone into the Western and Eastern branches. The axial lines of the branches are subparallel and change orientation conformably with the structures of the Ergalakh–Bystrinsk and Daldykan fault zones (Fig. 6). The Western branch is confined to the Daldykan Fault, lying among rocks of the Lower Devonian Razvedochninsk and Kureika formations, while the Eastern branch is located in the eastern limb of this fault. The thickness of the Lower Norilsk intrusion is 35–50 m on average. In general, it represents a low-angle sill that is conformable with the general dip of the sedimentary beds. In the bulges, the intrusion acquires a tube-like shape within increasing thickness up to 150–230 m (Fig. 6). The bottom of the intrusion plunges to the Lower Devonian Zubov Formation.

The Zelenaya Griva intrusion is confined to the southern and southwestern surrounding of the Norilsk depression (Figs. 1, 7a, 7b). The position of the intrusion is controlled by the Norilsk–Kharaelakh fault and subsidiary Rudninsk Fault, as well as by the transverse Kraevoy fault. The main plicative structures are the Uboininsk uplift and Zelenaya Griva basin, which NW orientation coincides with the strike of the Rudninsk fault. The intrusion is localized in rocks of the C_2–P_3 Tunguska Group and has a sheet morphology from 24 to 200 m thick with bulges and pinches.

METHODS

The compositions of rocks and ore mineralization were studied by petrographic and mineralogical methods. The chemical composition of minerals was analyzed on a JXA-8200 JEOL microprobe at the Center for Collective Use IGEM-Analitika. The rare-earth elements were determined using an inductively coupled plasma mass spectrometer XSeries 2 Thermo Scientific at the IGEM RAS.

The isotope composition and concentrations of Rb, Sr, Sm, and Nd in the rocks were analyzed using a Finnigan MAT TRITON TI at the Centre of Isotopic Research (CIR) of the Karpinsky Russian Geological Research Institute (VSEGEI), St. Petersburg. The S isotope composition was analyzed using a DELTAplusXL mass spectrometer equipped with EA-ConFlo III at the CII VSEGEI and a FlashEA HT 1112 spec-

[1] Supplemetary materials for the Russian and English on-line versions of the paper at https://elibrary.ru/ and http://link.springer.com/ , are presented in Supplementary 1:
ESM_1.pdf: Methods;
ESM_2.pdf: Compositional variations of minerals throughout the vertical section;
ESM_3.pdf: Position of the Lower Talnakh intrusion in the northwest-southeast section of the Talnakh ore field;
ESM_4.pdf: Position of the Lower Talnakh intrusion in the NNW–SSW sub-meridional section of the Talnakh intrusion;
ESM_5.pdf: Textures of rocks of the Lower Talnakh intrusion in the ZF-211 drill hole core;
ESM_6.pdf: Compositions of minerals in rocks of the Lower Talnakh type intrusions;
ESM_7.pdf: Whole rock compositions of the Lower Talnakh type intrusions compared to the whole rock compositions of other magmatic complexes of the Norilsk region;
ESM_8.pdf: Hafnium isotope composition for zircons from intrusions of the Norilsk region;
ESM_9.pdf: Compositions of rock-forming minerals of the Lower Talnakh intrusion (drill hole TG-31);
ESM_10.pdf: Compositions of rock-forming minerals of the Lower Talnakh intrusion (drill hole OP-4);
ESM_11.pdf: Compositions of rock-forming minerals of the Lower Norilsk intrusion (drill hole NP-37);
ESM_12.pdf: Composition of rock-forming minerals of the Zelenaya Griva intrusion (drill hole F-233);
ESM_13.pdf: Whole rock compositions of the Lower Talnakh type intrusions;
ESM_14.pdf: REE distribution in rocks of the Lower Talnakh and Zelenaya Griva intrusions;
ESM_15.pdf: Rb-Sr isotope data for rocks of the Lower Talnakh, Zelenaya Griva and Lower Norilsk intrusions;
ESM_16.pdf: Rb-Sr isotope data for rock-forming minerals of the Lower Talnakh intrusion (drill hole TG-31);
ESM_17.pdf: Sulfur, base metals and PGE abundances in rocks of the Lower Talnakh type intrusions;
ESM_18.pdf: Composition of sulfides in rocks of the Lower Talnakh type intrusions;
ESM_19.pdf: S and Cu isotope composition of sulfides in the Lower Talnakh type intrusions.

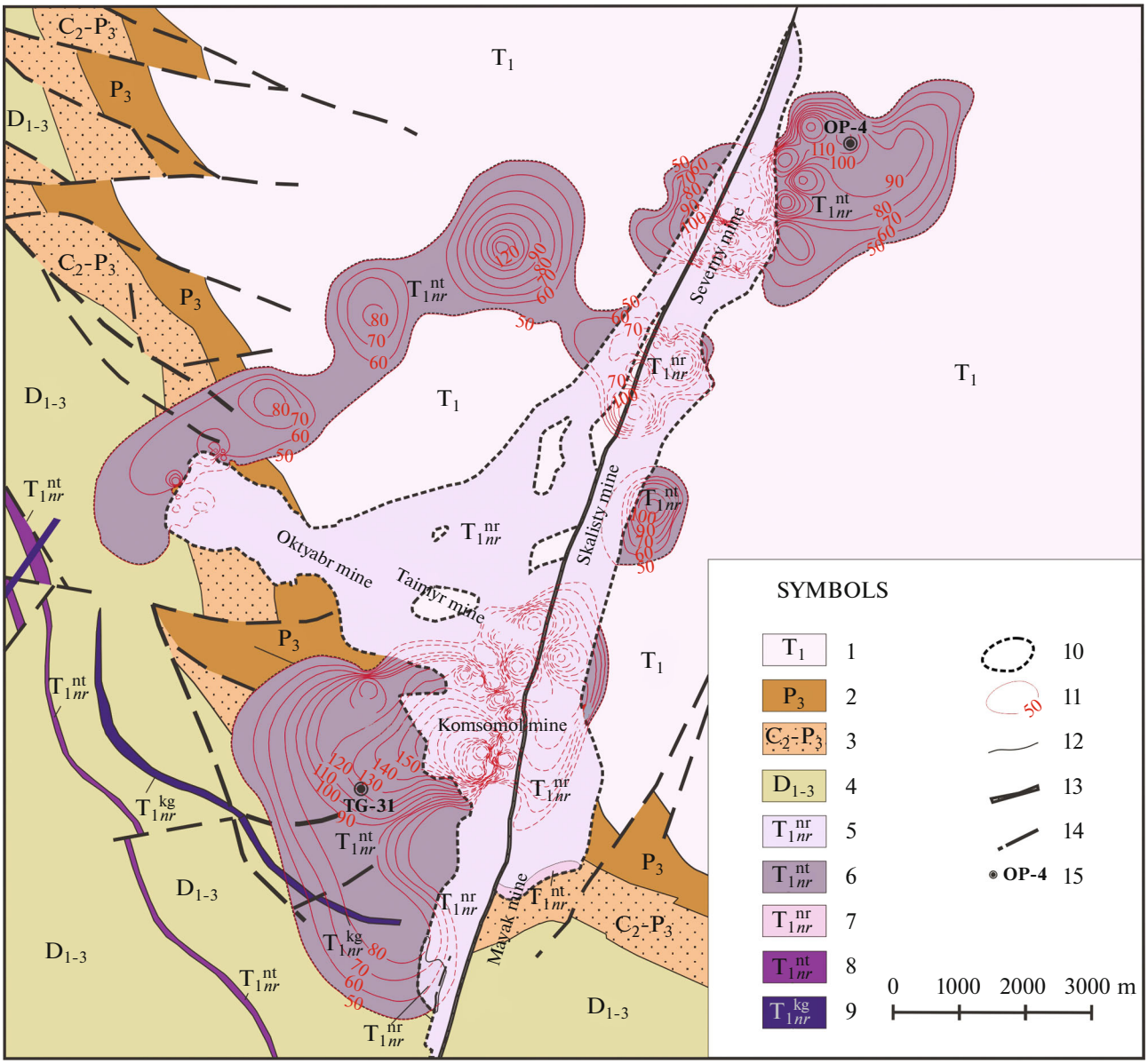

Fig. 2. Geological map of the Talnakh ore cluster (compiled by geologists of JSC Norilskgeologiya, simplified and partially modified). (1, 2) volcanogenic rocks: (1) Lower Triassic: Kharaelakh, Mokulai, Morongo, Nadezhda, Khakanchan, Gudchikha, and Syverma formations, (2) Upper Permian: Ivakin Formation; (3) Upper Carboniferous–Upper Permian: Tunguska Group; (4) Lower–Upper Devonian: Yampakhty, Khrebtov, Zubov, Kureika, Razvedochninsk, Mantur, Yukta, Nakokhoz, Kalargon, and Fokina formations; (5–6) Lower Triassic intrusions: (5) Norilsk type, chonolith-like differentiated bodies, (6) Lower Talnakh type, chonolith-like differentiated bodies; (7–9) exposures of the intrusions beneath the Quaternary deposits: (7) Norilsk, (8) Lower Talnakh, (9) Kruglogorka type; (10) outlines of the Norilsk type ore-bearing intrusions; (11) isopachs of the Lower Talnakh intrusion at its thickness over 50 m; (12) geological boundaries; (13) Norilsk–Kharaelakh fault; (14) faults; (15) drill holes and their numbers.

trometer at the Laboratory of Isotope Geochemistry and Geochronology of IGEM RAS. The Cu isotope composition was measured using a Neptune Thermo Finnigan at the CIR VSEGEI and a Neptune Plus–Thermo Fisher at the Institute of Geology and Geochemistry of the Ural Branch of the Russian Academy of Sciences (IGG UB RAS), Yekaterinburg.

All techniques are described in ESM_1.pdf (Suppl. 1).

INNER STRUCTRUE OF THE INTRUSIONS AND ROCK PETROGRAPHY

Typical Structure of the Section

The Lower Talnakh type intrusions are divided into following units (from top downward):

1. The Upper gabbroic series of contact gabbrodolerites, hybrid metasomatic and contaminated rocks, prismatically granular olivine-free gabbrodolerites,

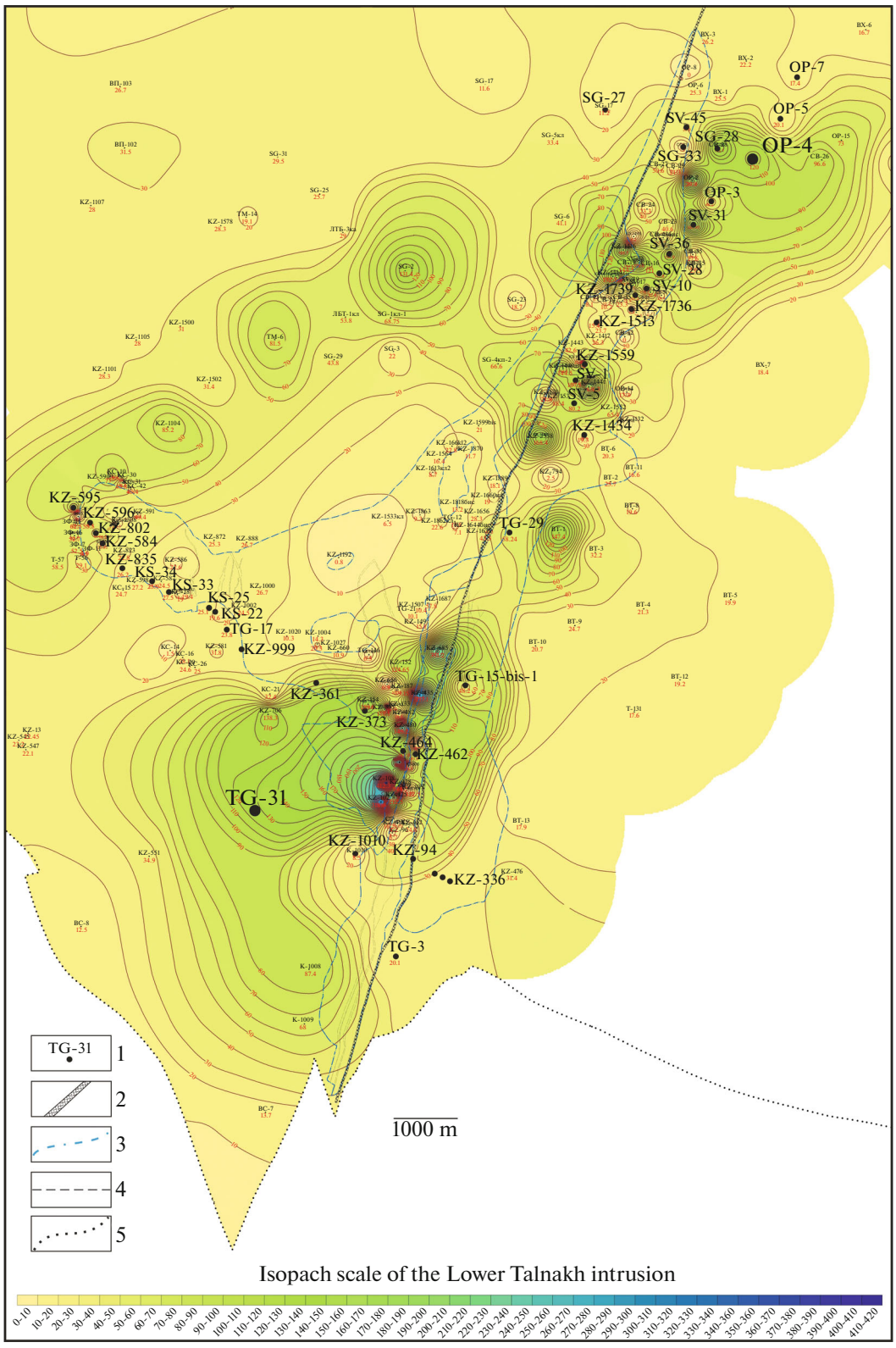

Fig. 3. Plan of isopachs of the Lower Talnakh intrusion. (1) drill hole numbers used to construct geological sections; (2) Norilsk–Kharaelakh fault; (3) other faults; (4) isopachs; (5) outlines of the Lower Talnakh intrusion.

gabbro-diorites, and chloritized, carbonated and albitized gabbrodolerites.

2. The Main differentiated series of olivine-free, olivine-bearing, olivine, and picritic gabbrodolerites and troctolites.

3. The Lower gabbroic series made up of taxitic-like, taxitic, and contact gabbrodolerites.

Gabbro-diorites and contaminated hybrid–metasomatic rocks are confined to the areas with significant thickness. In the areas of reduced thickness, these rocks occur as thin lenticular bodies and schlierens.

Hybrid–metasomatic rocks are developed after diorites and frequently contain xenoliths of sedimentary rocks. Rocks have prismatic-granular, granoblastic and heterogranoblastic texture. Major minerals are K–Na feldspars (40–70 vol %), plagioclase (20–30 vol %), hornblende, biotite, Ti-magnetite, titanite, and phlogopite. Plagioclase is replaced by albite, while clinopyroxene forms prisms and xenomorphic grains. Clinopyroxene is replaced by postmagmatic brown and green hornblende. Quartz (up to 5 vol %) frequently forms granophyric intergrowths with K-feldspar.

Gabbro-diorites represent a coarse-grained rock with prismatic-granular, ophitic, and poikiloophitic texture, which is made up of plagioclase laths and tablets (core An_{25-53}, rim An_{3-8}, ESM_10.pdf, ESM_12.pdf (Suppl.)) and euhedral to xenomorphic clinopyroxene (core Fs_{9-11}, rim Fs_{9-19}). Plagioclase is almost completely albitized, while clinopyroxene is amphibolized. Interstices are filled with quartz (up to 5 vol %), which frequently forms granophyric intergrowths with K-feldspar. Biotite accounts for 3–5 vol % and commonly intergrows with Ti-magnetite (3–5 vol %). Rock also commonly contains apatite, which forms acicular grains cutting across rock-forming minerals.

Olivine-free and olivine-bearing gabbrodolerites are of limited abundance, commonly being confined to thin portions of the intrusions and areas of its pinching out. In the intrusions with elevated thickness, they were found in the transition zone from the Upper gabbroic to the Main series (Figs. 8, 9). Rocks are prismatic-granular, ophitic, poikiloophitic in texture and consist mainly of plagioclase (An_{9-36}—core, An_{5-56}—rim, ESM_9.pdf–ESM_12.pdf (Suppl.)), which prismatic and tabular grains are replaced by albite and saussurite. Clinopyroxene (core Fs_{8-3}, rim Fs_{11-13}) contains 0.32–0.5 wt % TiO_2 and 0.02–0.37 wt % Cr_2O_3. It forms prismatic and anhedral interstitial grains and oikocrysts, which are replaced by green hornblende and chlorite. Olivine occurs sporadically (<5 vol %). Quartz is rarely observed in the interstices as separate grains and in the intergrowths with K-feldspar. Phlogopite in olivine-free gabbrodolerites has Mg# = 45–72 reaching Mg# = 75 in the olivine-bearing varieties. Ore mineral is Ti-magnetite.

The underlying horizon of olivine, picritic gabbrodolerites and troctolites, especially in the intrusions of the elevated thickness, composes the major part of sequence, amounting up to 75% of its thickness (Figs. 8, 9). In the areas of reduced thickness (<25–40 m), high-Mg rocks are absent, and the intrusions are composed of olivine-free and olivine-bearing gabbrodolerites. High-Mg rocks shows no clear differentiation, while different rocks types are related by gradual transitions without clear boundaries.

Olivine gabbrodolerites are mainly made up of plagioclase (35–45 vol %) and clinopyroxene (15–20 vol %). Rocks are poikiloophitic, poikilitic, and ophitic. Plagioclase (core An_{68-86}, rim An_{56-70}, ESM_9.pdf–ESM_12.pdf (Suppl.)) forms laths and wide tablets. Clinopyroxene (core Fs_{7-13}, rim Fs_{8-13}) forms xenomorphic oikocrysts, which include chadacrysts of plagioclase laths and olivine. The TiO_2 content in clinopyroxene is 0.34–1.28 wt %, while Cr_2O_3 content reaches 0.19 wt %. Olivine (core $Fo_{71-82.3}$, rim Fo_{70-83}) contains 0.01–0.2 wt % NiO and is represented by subhedral and xenomorphic grains. Orthopyroxene ($Fs_{19-25}Wo_{2-3}En_{72-78}$) and phlogopite (Mg# = 66–86) ubiquitously occur in subordinate amounts (<3–6 vol %). The orthopyroxene contains up to 1 wt % TiO_2 and up to 0.03 wt % Cr_2O_3, while phlogopite has widely varying TiO_2 content of 1.15–9.74 wt %. Clinopyroxene is replaced by hornblende, green amphibole, while olivine is replaced by serpentine and bowlingite. Ore minerals (1–2 vol %) are represented by Ti-magnetite and ilmenite.

Olivine-rich high-Mg rocks are subdivided into troctolites (>15 vol % olivine) and picritic gabbrodolerites (>30 vol % olivine), with the former having the lower clinopyroxene content of <10 vol % (Le Maitre et al., 2002). However, the troctolite layer shows a local increase in clinopyroxene to over 10 vol % without sharp lithological boundaries that is considered as clinopyroxene-enriched troctolite.

Troctolites of the Lower Talnakh type intrusions are usually enriched in clinopyroxene and have the following composition: olivine (15–50 vol %), plagioclase (25–50 vol %), clinopyroxene (5–10, up to 20 vol %), orthopyroxene (1–5, up to 10 vol %), and phlogopite (1–5, up to 10 vol %). Rock is porphyritic, poikiloophitic, and poikilitic. Numerous schlierens of other gabbroic rocks (olivine-free, olivine-bearing, and olivine gabbrodolerites) result in taxitic appearance of the rocks. Olivine (Fo_{76-83}) forms: (1) euhedral and round grains 0.1–1.8 mm in size, frequently as chadacrysts in clinopyroxene; (2) xenomorphic palmate grains up to 6 mm long, but mainly 1.0–1.5 mm, with inclusions of plagioclase laths and grains of clinopyroxene. The NiO content in olivine accounts for 0.03–0.10 wt % (ESM_9.pdf–ESM_12.pdf (Suppl.)). Clinopyroxene (core Fs_{8-11}, rim Fs_{8-19}) is developed as prismatic and xenomorphic oikocrysts up to 6 mm

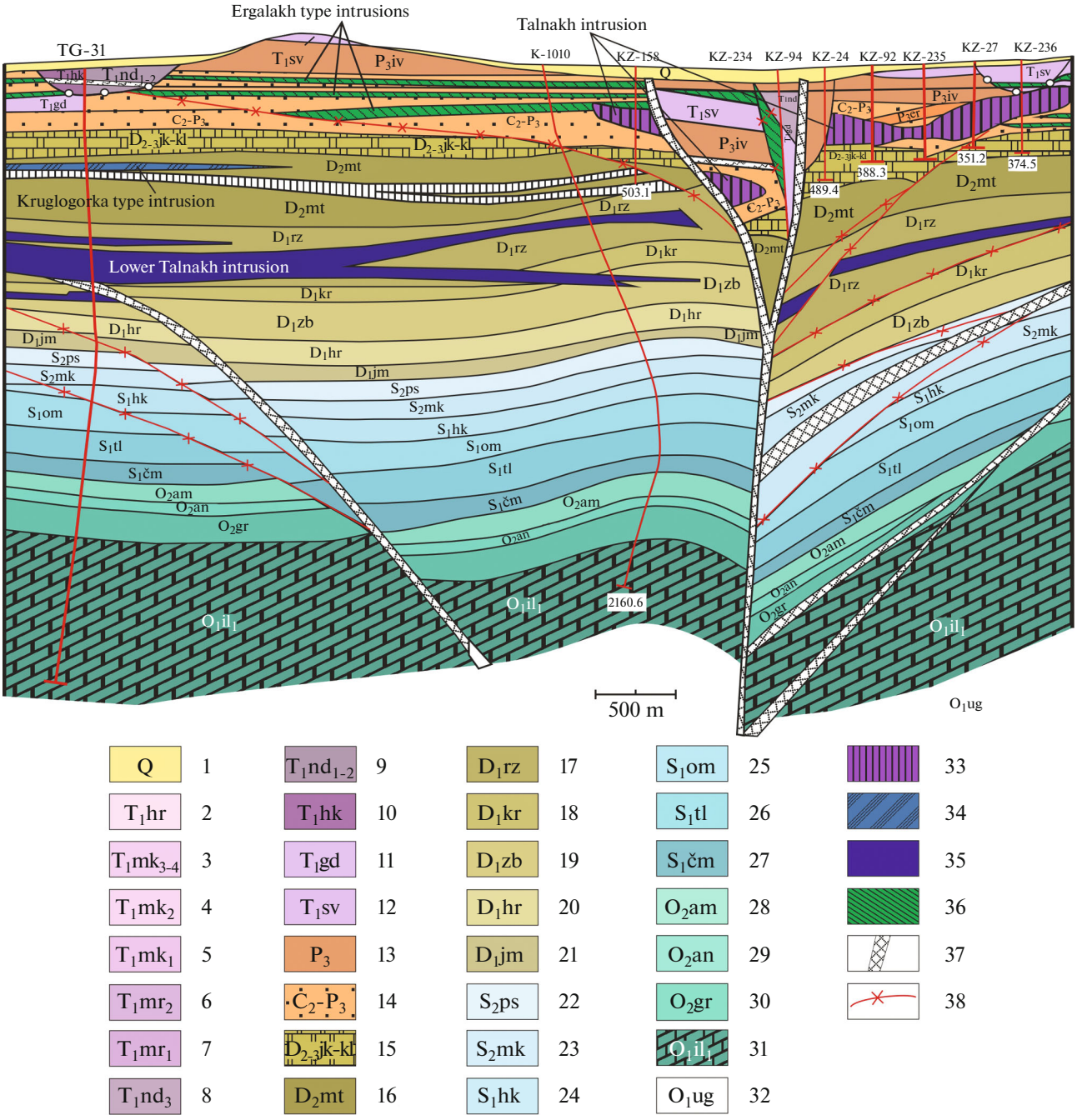

Fig. 4. Geological section of the southern area of the Talnakh ore field. (1) Quaternary deposits; (2) Kharaelakh Formation, (3) Mokulai Formation. Top pack; (4) Mokulai Formation. Middle pack; (5) Mokulai Formation. Bottom pack; (6) Morongo Formation. Upper unit; (7) Morongo Formation. Lower unit; (8) Nadezhda Formation. Upper unit; (9) Nadezhda Formation. Middle and lower units; (10) Khakanchan Formation; (11) Gudchikha Formation; (12) Syverma Formation; (13) Ivakin Formation; (14) Tunguska Group; (15) undivided Yukta, Nakokhoz, Kalargon formations; (16) Mantur Foramtion; (17) Razvedochninsk Formation; (18) Kureika Formation; (19) Zubov Formation; (20) Khrebtov Formation; (21) Yampakhty Formation; (22) Postnich Formation; (23) Makus Formation; (24) Khyukta Formation; (25) Omnutakh Formation; (26) Talikit Formation; (27) Chamba Formation; (28) Amorakan Formation; (29) Angir Formation; (30) Guragir Formation; (31) Il'tyk Formation; (32) Uigur Formation; (33–36) intrusive rocks: (33) Norilsk type, (34) Kruglogorka type, (35) Lower Talnakh type, (36) Ergalakh intrusive complex, (37) Norilsk–Kharaelakh fault; (38) other faults.

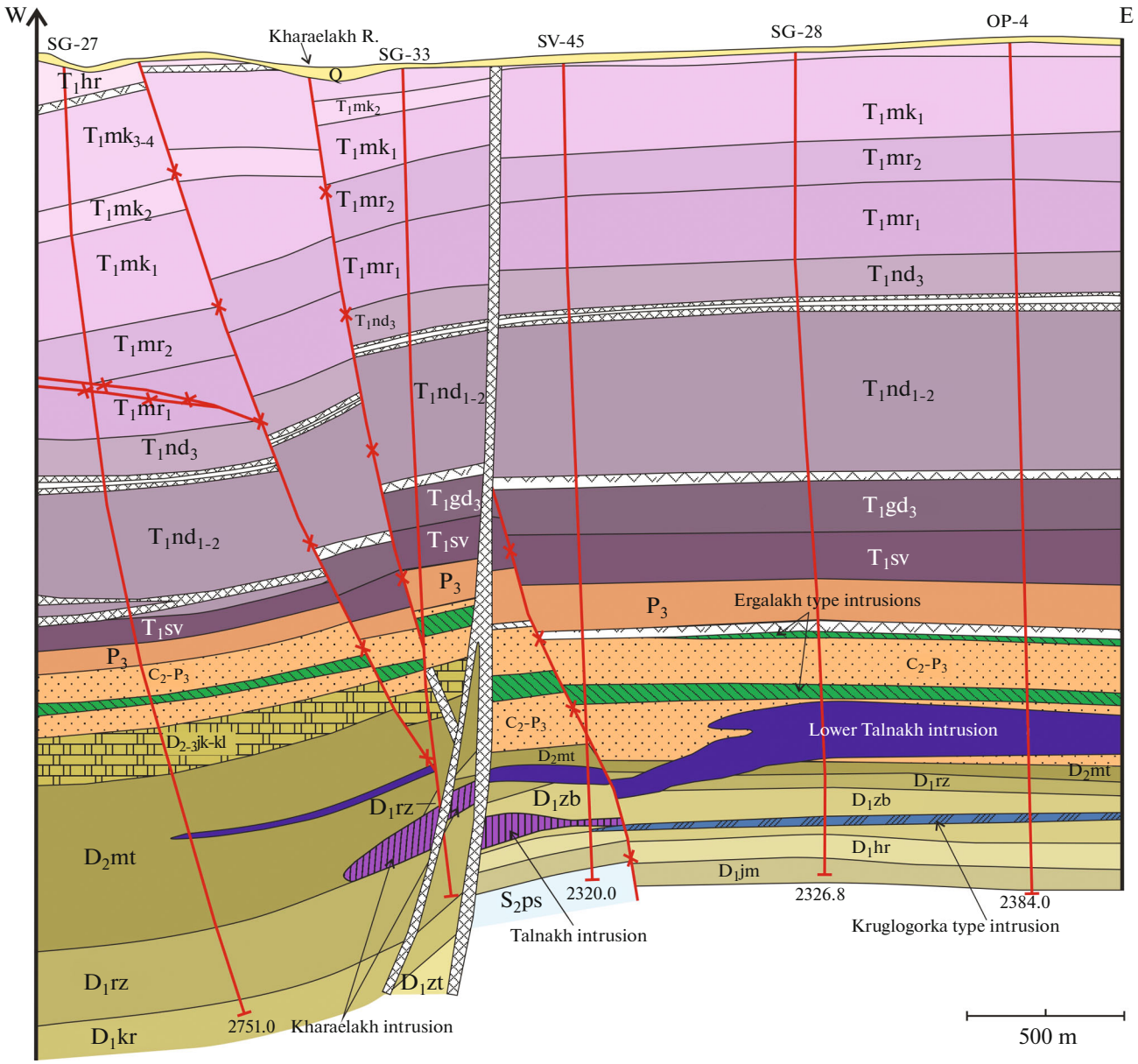

Fig. 5. Geological section of the northern (Olor) area of the Talnakh ore field. For symbols, see Fig. 4.

long with inclusions of plagioclase and olivine. The TiO_2 content in clinopyroxene is 0.30–0.50 wt %, Cr_2O_3, up to 0.38 wt % (ESM_9.pdf–ESM_12.pdf (Suppl.)). Plagioclase (core $An_{82–85}$, rim $An_{71–83}$) forms: (1) large (1.5–10 mm) tabular and prismatic grains, defining porphyritic texture; (2) laths 0.1–1.5 mm long, frequently as chadacrysts in clinopyroxene. Orthopyroxene ($Fs_{19–25}Wo_{2–3}En_{72–78}$), containing 0.12–0.62 wt % TiO_2 and up to 0.07 wt % Cr_2O_3 occurs mainly as rims around olivine and as prismatic grains. Phlogopite (Mg# = 73–82) contains 4.02–6.56 wt % TiO_2 and forms platelets up to 4 mm in the interstices and rims around ore minerals. Opaques (1–3 mm) are represented by Ti-magnetite, which is decomposed into magnetite and ilmenite, independent ilmenite, and less common fine grains of Cr-magnetite. Apatite forms long-prismatic grains and thin needles in biotite.

Olivine is replaced by serpentine, talc, bowlingite (a mixture of smectite group minerals and serpentine), with magnetite exsolution. Clinopyroxene is replaced by green hornblende and chlorite. Plagioclase is prehnitized and saussuritized. In some areas, especially in the Lower Talnakh intrusion, the unaltered troctolites could alternate with pyroxene and anhydrite–pyroxene metasomatites and marbles after mudstones, marls, and carbonates, with metasomatites accounting for up to 50% of intrusion thickness.

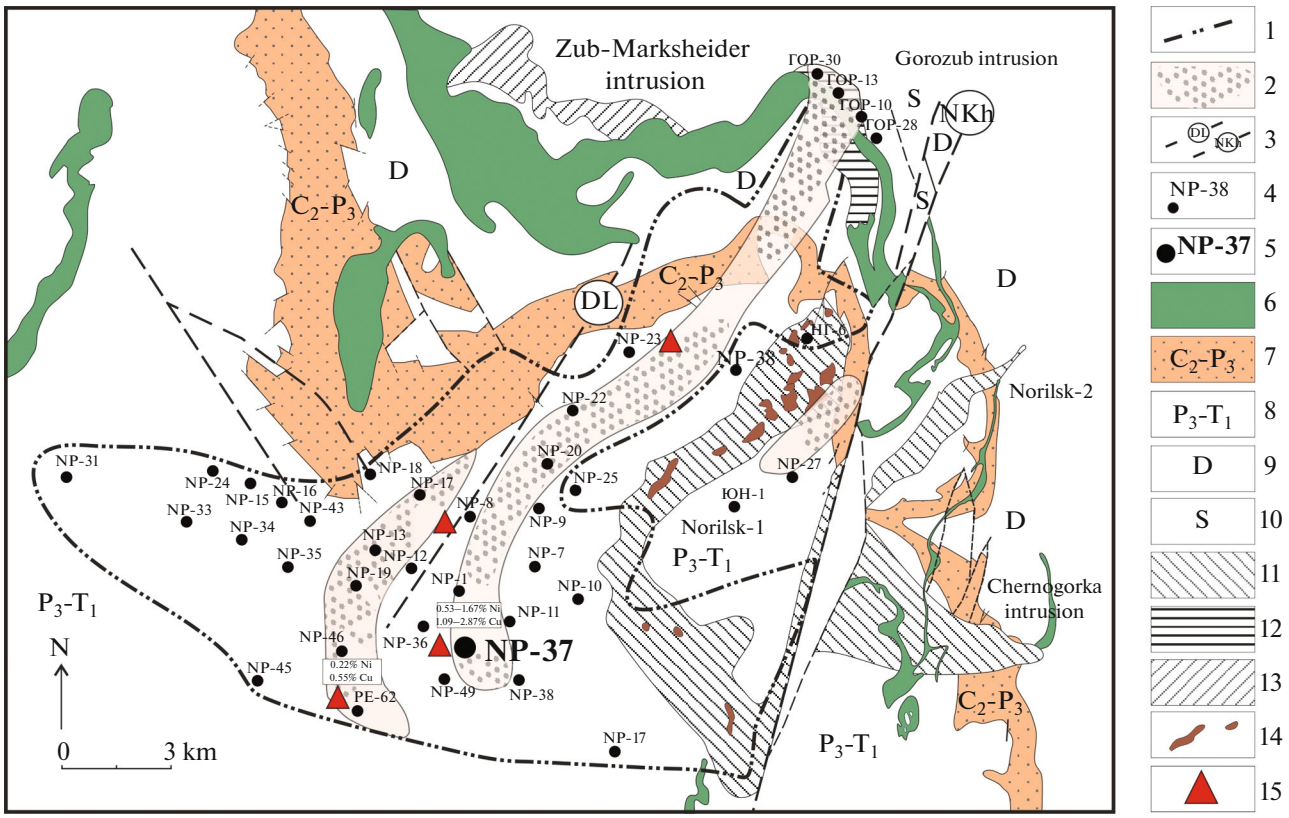

Fig. 6. Geological-structural scheme of the Lower Norilsk intrusion. (1) inferred extension area of the Lower Norilsk intrusion; (2) extension area of picritic gabbrodolerites; (3) faults: (DL) Daldykan, (NKh) Norilsk–Kharaelakh; (4) drill hole numbers; (5) drill hole NP-37, core throughout the Lower Norilsk intrusion was sampled for petrological-geochemical and isotope-geochemical studies; (6) Daldykan complex; (7) Upper Carboniferous–Upper Permian. Tunguska Group: coaliferous terrigenous–sedimentary rocks; (8) Upper Permian–Lower Triassic. Tuff lava sequence; (9) Devonian system. Terrigenous–carbonate rocks; (10) Silurian. Carbonate rocks; (11) ore-bearing intrusions (Norilsk-1, Norilsk-2, Chernogorka); (12) Gorozub intrusion; (13) Zubov-type intrusion; (14) extension areas of high grade Cu–Ni ores; (15) drill holes with intervals of elevated sulfide contents.

Picritic gabbrodolerites do not occur continously in all sections of the Lower Talnakh type intrusions, forming mainly interlayers among troctolites and olivine gabbrodolerites in swells and near axial line of the massifs (Figs. 8, 9). Rocks have poikiloophitic, poikilitic, ophitic, and segregation textures (ESM_5.pdf (Suppl.)).

Rock is dominated by olivine (30–60 vol %) with $Fo_{76–83}$ core and $Fo_{74–81}$ rim (ESM_9.pdf–ESM_12.pdf (Suppl.)), which forms euhedral and oval grains 0.1–1.5 mm in size, as well as xenomorphic palmate grains of 1–2 mm in size. The NiO content in olivine accounts for 0.06–0.13 wt %. Clinopyroxene (15–30, up to 45 vol %) forms xenomorphic oikocrysts up to 8 mm in size with chadacrysts of plagioclase laths and subhedral olivine grains. In some areas, pyroxene is highly saturated in olivine such that only marginal parts of oikocrysts are seen. The clinopyroxene corresponds to augite (core $Fs_{6–10}$, rim $Fs_{8–11}$) (ESM_9.pdf–ESM_12.pdf (Suppl.)) with 0.20–0.82 wt % TiO_2 and up to 0.47 wt % Cr_2O_3. Plagioclase (10–45 vol %) forms porphyritic grains over 2 mm in size (core $An_{70–86}$, rim $An_{60–84}$), while cumulus crystals are 1–2 mm in size and laths in interstices are 0.1–1 mm in size. Large plagioclase grains could contain inclusions of euhedral olivine. Phlogopite (Mg# = 76–90, 0.24–6.77 wt % TiO_2) accounts for 3–7 vol %. Peritectic orthopyroxene around large olivine grains is more magnesian ($En_{67–84}$) than olivine. Ore oxides are represented by xenomorphic decomposed Ti-magnetite and lamellar ilmenite.

Plagioclase is replaced by saussurite and chlorite. Clionyroxene is replaced by actinolite, while olivine - by serpentine and magnetite. Both troctolites and picritic gabbrodolerites locally contain disseminated, interstitial, and globular layered sulfides, which are similar to those typical of the picritic layers of the Norilsk type intrusions (Fig. 5a in ESM_5.pdf (Suppl.)).

Taxitic and taxitic-like gabbrodolerites did not receive the wide distribution and occur in the sections with highest thickness. Such layers are no more than 10–15 m thick and confined mainly to the basal parts of the intrusions, although occur also in the central

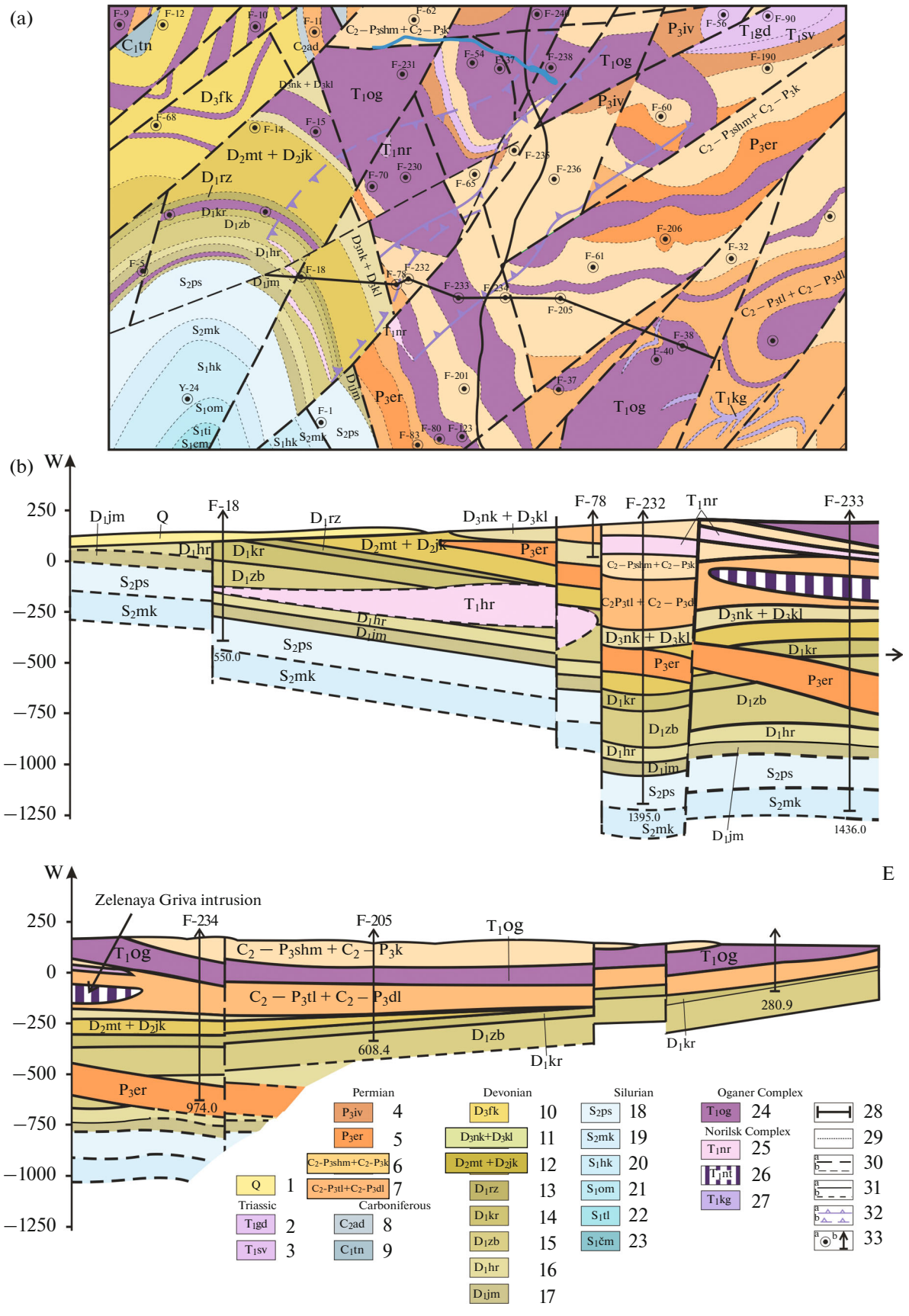
(a)
C1tn
C2ad
D3fk
D3nk + D3kl
T1og
D2mt + D2jk
D1rz
D1kr
D1zb
D1hr
D1jm
S2ps
S2mk
S1hk
S1om
S1ti
S1čm
T1nr
P3er
P3iv
T1gd
T1sv
C2 – P3shm + C2 – P3k
C2 – P3tl + C2 – P3dl
T1kg
I
(b)
W
E
Zelenaya Griva intrusion
550.0
974.0
608.4
1395.0
1436.0
280.9
Permian
Triassic
Carboniferous
Devonian
Silurian
Oganer Complex
Norilsk Complex

Fig. 7. Geological map of the site of the Sredne-Fokina area (a), compiled by geologists of JSC Norilskgeologiya and geological section of the Sredne-Fokina area along line I–I (b). (1) Quaternary deposits; (2–3) Triassic system T_1: (2) Gudchikha Formation, (3) Syverma Formation; (4–7) Permian–Triassic P_3–T_1: (4) Ivakin Formation, (5) Ergalakh Complex; (6–9) Carboniferous–Permian Tunguska Group C_2–P_3: (6) Shmidtinsk and Kaierkan formations; (7) Talnakh and Daldykan formations; (8) Adylkan Formation, (9) Tundra Formation; (10–17) Devonian system: (10) Fokina Formation, (11) Nakokhoz and Kalargon formations; (12) Mantur and Yukta formations; (13) Razvedochninsk Formation, (14) Kureika Formation, (15) Zubov Formation, (16) Khrebtov Formation, (17) Yampakhty Formation; (18–23) Silurian System: (18) Postnich Formation. Dolomites, clay dolomites, anhydrites, anhydrite–dolomite rocks, (19) Makus Formation, (20) Khyukta Formation, (21) Omnutakh Formation, (22) Talikit Formation, (23) Chamba Formation, (24) Oganer Complex; (25–27) Norilsk complex: (25) Norilsk type, (26) Lower Talnakh type, (27) Kruglogorka type; (28) line of geological section; (29) geological boundaries; (30) faults: (a) main, (b) subsidiary; (31) outlines of the Lower Talnakh type intrusions at the depth: (a) inferred, (b) proved; (32) contour of the distribution of the Norilsk type intrusions at depth: (a) inferred, (b) proved; (33) drill holes: (a) in a plan view, (b) on section.

parts of sections. Unlike taxitic gabbrodoleites of the ore-bearing massifs, the taxitic texture in these rocks is weakly expressed (Figs. 5b, 5c in ESM_5.pdf (Suppl.)). It is caused by the appearance of leucocratic schlierens and fragments dominated by plagioclase, including monomineral segregations of plagioclases from glomeroporphyritic intergrowths to large schlierens, and fragments of finer grained rocks enriched in clinopyroxene, frequently overgrown by coarse-grained plagioclase. These schlierens and fragments vary from tenths to tens of centimeters in size, and their boundaries could be sharp (Fig. 5b in ESM_5.pdf (Suppl.)) and obscured (Fig. 5c in ESM_5.pdf (Suppl.)) in different intervals, thus reflecting the different degree of resorption of their margins. The rock textures in matrix and fragments are widely variable: poikilitic, poikiloophitic, ophitic, prismatically granular, and pegmatoid ones. Based on the composition, taxitic gabbrodolerites correspond to olivine-bearing and olivine gabbrodolerites, at uneven distribution of plagioclase (40–50 vol %), clinopyroxene (25–30 vol %), olivine (1–20 vol %), phlogopite (1–3 vol %) and orthopyroxene (a few percents). Cumulus assemblage is represented by olivine, plagioclase, and clinopyroxene unlike those of the Norilsk type intrusions, where olivine is scarce and occurs only in the upper parts of the lower taxitic gabbrodolerites near their contacts with picritic gabbrodolerites.

Olivine ($Fo_{75–79}$, ESM_9.pdf–ESM_12.pdf (Suppl.)) forms: (1) euhedral grains up to 2 mm in size; (2) large (up to 5 mm) xenomorphic palmate grains with inclusions of plagioclase laths; (3) smaller (0.05–0.1 mm and less) grains of granulated olivine that forms irregularly shaped and veinlet-like aggregates. The NiO content in xenomorphic and euhedral olivine is 0.086–0.11 wt % and that of fine-grained olivine is 0.03–0.05 wt %. Clinopyroxene forms large (up to 3 cm) poikilocrysts with inclusions of prismatic plagioclase and euhedral grains of olivine, and grain in a finer-grained ophitic pyroxene–plagioclase groundmass. Clinopyroxene is zoned (core $Fs_{7–9}$, rim $Fs_{10–11}$) and contains 0.35–0.52 wt % TiO_2 and 0.09–0.94 wt % Cr_2O_3. Plagioclase (An_{75}) is developed as large (up to 1 cm, more frequently, 2–4 mm) poikilitic grains and small (0.1–0.5 mm) laths in the groundmass. Phlogopite has a magnesian composition (Mg# = 76–81). Opaques are Ti-magnetite, ilmenite; apatite occurs as an accessory mineral.

Plagioclase is replaced by prehnite and saussurite; clinopyroxene—by amphibole and chlorite, while olivine by serpentine and talc.

Thus, taxitic rocks of the Lower Talnakh intrusions, although distinguished by a clear clastic character of fragments, differ from taxitic rocks of the ore-bearing intrusions in the well expressed cumulate nature of matrix, where predominant assemblage is represented by olivine, plagioclase and clinopyroxene with later heteroadcumulate (poikilitic) textures formed during prolonged crystallization of olivine and pyroxene. In addition, taxitic gabbrodolerites of the Lower Talnakh intrusions are comparatively depleted in sulfides although within narrow intervals the content of sulfides could reach 30 vol % (Fig. 5d в ESM_5.pdf (Suppl.)).

Lower contact gabbrodolerites represent fine-grained rocks with poikiloophitic, ophitic, and doleritic texture and are developed almost in all sections of the intrusions although in some sections ultramafic rocks rest directly on rocks of the footwall. Plagioclase (25–45 vol %) (core $An_{68–82}$, rim $An_{27–74}$) forms tabular, prismatic, lath-like, and xenomorphic grains up to 2 mm in size. Clinopyroxene (25–35 vol %) is represented by oikocrysts and equant grains of augite ($Fs_{8–13}$ – core), which contain 0.35–0.50 wt % TiO_2 and 0.03–0.36 wt % Cr_2O_3. Olivine in form of euhedral and rounded grains accounts for up to 25 vol %, while magnesian phlogopite (Mg# = 72)—for 4 vol %. Ti-magnetite (no more than 2–3 vol %) occurs together with lamellar ilmenite.

Clinopyroxene is replaced by amphibole and chlorite, while plagioclase—by prehnite and saussurite, and olivine—by bowlingite and serpentine.

Compositional variations in minerals throughout the vertical section are given in ESM_2.pdf (Suppl.).

PETROCHEMISTRY AND GEOCHEMISTRY

Variations of Major Components

In terms of silica and alkali ($Na_2O + K_2O$) contents, rocks plot in the fields of the mesocratic and leucocratic ore-bearing intrusions of the Norilsk and

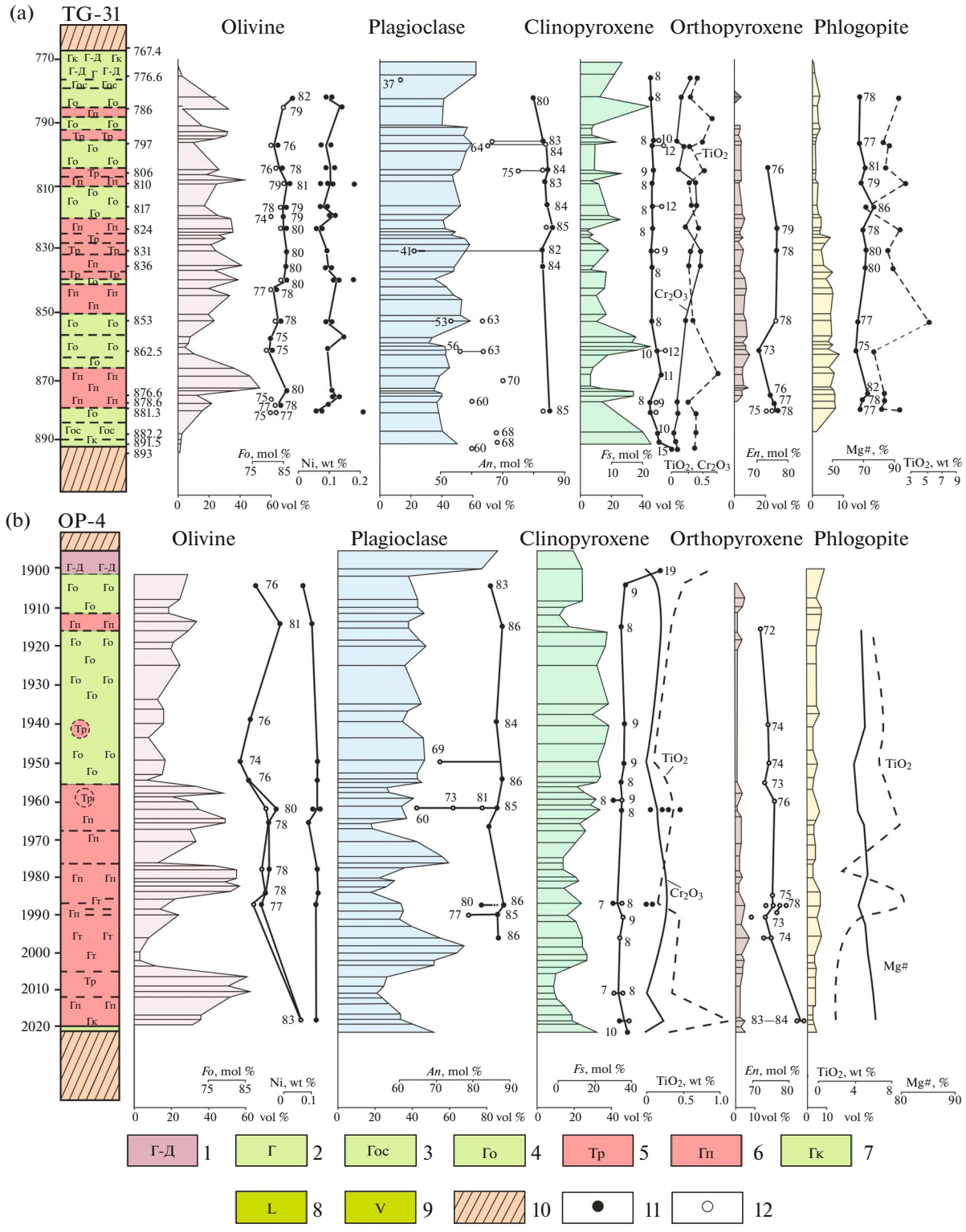

Fig. 8. Variations of contents and compositions of rock-forming minerals in sections of the Lower Talnakh type intrusion: (a) drill hole TG-31, (b) drill hole OP-4. (1) gabbro-diorites; (2–4) gabbrodolerites: (2) olivine-free, (3) olivine-bearing, (4) olivine; (5) troctolites; (6) picritic gabbrodolerites; (7) contact gabbrodolerites; (8) dolerites; (9) altered gabbrodolerites; (10) host rocks; (11) core of mineral; (12) rim of mineral.

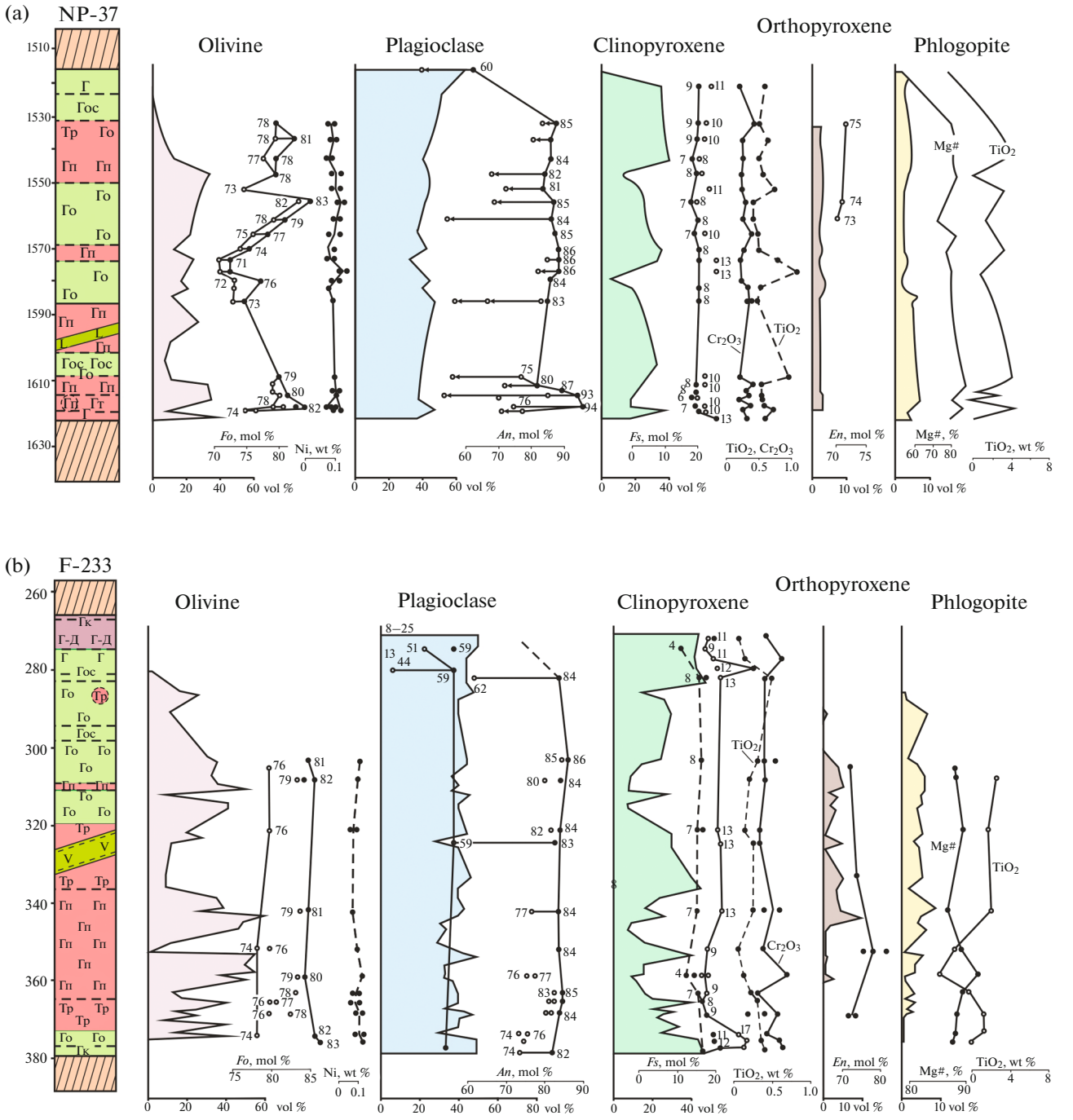

Fig. 9. Variations of contents and compositions of rock-forming minerals in sections of (a) Lower Norilsk (drill hole NP-37) and (b) Zelenaya Griva (drill hole F-233) intrusions. For symbols, see Fig. 8.

Zubov types. The SiO_2 content systematically decreases from rocks of the Upper gabbroic series to olivine rocks of the Main layered series (Figs. 8, 9) from 45.28–51.07 wt % in gabbrodiorites to 39.56–45.61 wt % in picritic gabbrodolerite (ESM_13.pdf (Suppl.)).

The MgO content increases in olivine-rich rocks, which occur throughout the entire section becoming more abundant in the lower half of the section. In gabbrodiorites and olivine-free gabbrodolerites, the MgO content is 3.50–8.70 wt % increasing downwards from 8.70–9.00 wt % in olivine-bearing to 11.03–26.65 wt % in picritic gabbrodolerites. The alkali content decreases in the same direction from gabbrodiorites and olivine-free gabbrodolerites (Na_2O 1.17–3.36 wt %, K_2O 0.28–1.15 wt %) to the picritic varieties (Na_2O

0.13–1.41 wt %, K_2O 0.09–1.08 wt %). The alkali content, however, could be modified by secondary alterations, mainly by albitization and therefore does not necessarily reflects their primary distribution.

The highest Ti and P contents were found in rocks of the Upper gabbroic series (0.63–4.18 wt % TiO_2 and up to 1.43 wt % P_2O_5), while their lowest contents are found in picritic gabbrodolerites (0.29–0.71 wt % TiO_2 and 0.02–0.14 wt %. P_2O_5).

The characteristic feature of rocks of the Lower Talnakh type intrusions is the low Cr_2O_3 content of 0.002–0.051 wt % (ESM_13.pdf (Suppl.)), which makes them different from rocks of the other complexes except for the Morongo suite. In the MgO–Cr_2O_3 diagram (Fig. 7a in ESM_7.pdf (Suppl.)), the rock compositions form a near-horizontal trend showing an insignificant rise of the Cr_2O_3 content with increasing MgO from 10 to 27 wt % that is consistent with the absence of Cr–Mg correlation in the sections (Fig. 10). This is caused by the absence of Cr own cumulus phases, while its balance is determined by the accumulation in clinopyroxene, which proportion in olivine cumulates decreases. At the same time, Cr accumulation can be illustrated in a Cr/Ti versus Mg# differentiation index diagram (Fig. 7b in ESM_7.pdf (Suppl.)), showing that the Cr/Ti ratio tends to increase with increasing Mg#, in the most primitive rocks with Mg# = 74–86 in particular. This correlation is caused by a decrease in Ti with increasing Mg# and reflected in the contrasting behavior of Cr and Ti during clinopyroxene crystallization.

Rare-Earth Element Distribution

The rare-earth element contents in rocks of the Lower Talnakh intrusions are given in ESM_14.pdf (Suppl.), while Fig. 11a (I, II, III) shows their C1 chondrite-normalized REE distribution patterns (McDonough and Sun, 1995) compared to those of the main rock types of the ore-bearing Kharaelakh intrusion (Fig. 11a (IV)). LREE shows the highest fractionation with La/Sm = 2–4.7 (Fig. 11b). The low Gd/Yb < 2 and their narrow variations are also typical of the other types of the intrusive complexes of the region, as well as of low-Ti volcanic rocks of the Norilsk region, but significantly differ from the elevated values typical of high-Ti and subalkaline basalts (Fig. 11b) (Lightfoot et al., 1994; Naldrett et al., 1995; Fedorenko, 2010). The gabbrodiorites and the lower contact gabbrodolerites are characterized by the elevated REE contents whereas a negative Eu anomaly is typical of all the rock types (Fig. 11a).

ISOTOPE-GEOCHEMICAL CHARACTERISTICS OF ROCKS

The Lower Talnakh intrusions are characterized by the highest values of initial Sr isotope composition $^{87}Sr/^{86}Sr$ (Sr_i) compared to the economic ore-bearing and mineralized intrusions of the Norilsk and Zubov types. The Sr_i values for rocks calculated for an age of 250 Ma vary from 0.7073 to 0.7087 (Fig. 12a; ESM_15.pdf (Suppl.)). Similar Sr_i values (from 0.7067 to 0.7087) were found in plagioclase and pyroxene (Fig. 12a; ESM_16.pdf (Suppl.)). The values of $\varepsilon_{Nd}(T)$ for the Lower Talnakh intrusions (from –1.8 to –5.9) are the lowest ones (enriched in the radiogenic component) among all the mafic–ultramafic massifs of the Norilsk region (Fig. 12a). Similar values of $\varepsilon_{Nd}(T)$ from –2.5 to –5.2 were determined in plagioclase and pyroxene throughout the entire section (Fig. 12a). Variations of the positive values of $\varepsilon_{Nd}(T)$ for olivine within 1.5–4.3 are not correlated with those of the host rocks (Fig. 12a), and their contribution in the whole rock characteristics is not obvious, in spite of the high olivine content (>10 vol %) in the studied samples. In the binary diagram Sr_i–$\varepsilon_{Nd}(T)$, the Lower Talnakh intrusions occupy a specific field, which does not overlap with the field of the economic ore-bearing and mineralized intrusions (Fig. 12b).

Zircons from the Lower Talnakh type intrusions have the lowest $^{176}Hf/^{177}Hf$ and $\varepsilon_{Hf}(T)$ (from 0.28239 to 0.28279 and from –7.4 to +5.6, respectively; ESM_8.pdf (Suppl.)) compared to zircons from the ore-bearing and mineralized intrusions of the Norilsk and Zubov types, which Hf isotope composition indicates the contribution from depleted mantle. A relatively nonradiogenic Hf isotope composition in zircons from the Lower Talnakh type intrusions suggests a significant crustal contribution at their formation (Malitch et al., 2009, 2018).

SULFIDE MINERALIZATION

Chemical and Mineral Compositions

Rocks of the Lower Talnakh type massifs have low concentrations of base metals (Ni—0.077–0.21 wt %, Cu—0.05–0.38 wt % (Figs. 7c, 7d in ESM_7.pdf (Suppl.)), which only locally increase up to 0.91 wt % Ni and 1.88 wt % Cu (ESM_17.pdf (Suppl.)) in the lower portions of the Lower Norilsk and Lower Talnakh intrusions. For comparison, disseminated ores of the Talnakh intrusion contain mainly 0.42–0.92 wt % Ni and 0.64–1.38 wt % Cu, while those of the Norilsk-1 intrusions are within 0.23–1.20 wt % Ni and 0.18–2.20 wt % Cu. The Ni/Cu ratio is equal to 0.55–1.4 (up to 6.0) in the Lower Talnakh type massifs, whereas it varies within 0.32–0.56 and 0.65–0.80 in disseminated ores of Talnakh and Norilsk-1 respectively, which emphasizes the depletion of the Lower Talnakh type rocks in Cu relative to Ni. In contrast, the Co concentration in the Lower Talnakh type massifs is 50–270 ppm, where 50 ppm is the detection limit, while the Co (ppm)/S (wt %) ratio varies within 60–350 (up to 600). In disseminated ores of the ore-bearing intrusions, the Co/S ratio varies within 19–71 at a

wider range of Co content from 50 to 1400 ppm. Thus, in recalculation to 100% sulfides, mineralized Lower Talnakh type sulfides are enriched in Co that is mineralogically expressed in the elevated content of this metal in pentlandite (up to 10 wt % Co).

The concentration of noble metals in the Lower Talnakh type massifs is extremely low compared to the other types of the Norilsk intrusive complex. The total PGE content (Pt + Pd + Rh + Ir) is 0.03–0.26 up to 0.40 ppm not exceeding 0.19 ppm even in sulfide-rich areas (0–40 vol % sulfides) (ESM_17.pdf (Suppl.)), whereas their contents in Talnakh and Norilsk-1 disseminated ores exceed 10 and 26 ppm, respectively. Recalculated to 100% sulfides, the PGE concentration in the Lower Talnakh type intrusions is also lower: the PGE (ppm)/S (wt %) ratio is within 0.08–0.26 rarely reaching 0.46, i.e., PGE tenor (PGE content in 100% sulfides) does not exceed 16 ppm. For comparison, the PGE (ppm)/S (wt %) ratio varies from 0.81 to 1.5 in Talnakh disseminated ores and from 1 to 3.5 and from 3.5 to 8.5 in those of the Norilsk-1 and Chernogorka deposit that corresponds to the PGE tenor within 28–52, 35–120, and up to 300 ppm, respectively. Mineralized rocks of the Lower Talnakh intrusions have Pt/Pd = 0.07–0.47 compared to Pt/Pd = 0.25–0.45 for disseminated PGE–Cu–Ni ores.

Sulfide mineralization is mainly confined to the high-Mg horizons made up of picritic gabbrodolerites, troctolites, and, to lesser extent, olivine gabbrodlerites. Sulfides are mainly accumulated in swells. In thinner bodies and apophyses, sulfides are either absent or occur in insignificant amounts (<1 vol %).

Sulfides in the mineralized zones of the Lower Talnakh type intrusions commonly account for 0.5–3.5, although to 5–10% in separate areas and up to 30–40% in some basal portions of the Lower Norilsk intrusion. Sulfides form small (up to 2, more rarely, up to 4 mm) interstitial aggregates, which shape is determined by outlines of surrounding silicates, as well as occur as rounded globules and lens-like blebs 5–30 mm in size. The latter are layered into pyrrhotite in the lower part and chalcopyrite in the upper part, as observed in globular sulfides of the picritic horizons of the Norilsk type deposits, and most frequently are restricted to the picritic horizons in the lower parts of the intrusions. Veinlets and lenses of massive sulfide ores up to 20 cm thick made up mainly of pyrrhotite occur rarely (Fig. 7).

Sulfide mineralization is represented by three paragenetic associations: (1) hexagonal pyrrhotite + chalcopyrite + pentlandite; 2) troilite ± hexagonal pyrrhotite + Fe-rich pentlandite + Fe-rich chalcopyrite (putoranite $Cu_9(Fe,Ni)_9S_{16}$, talnakhite $Cu_9(Fe,Ni)_8S_{16}$) ± cubanite $CuFe_2S_3$), and (3) monoclinic pyrrhotite + chalcopyrite + Ni-rich pentlandite (ESM_18.pdf (Suppl.))

The first association is typical of the upper and lower portions of the intrusions, the second association occurs in olivine-rich rocks, and the third association is found in sulfide mineralization in host rocks and in the inner endocontact of the intrusions. In the Zelenaya Griva intrusion, unlike the Lower Talnakh and Lower Norilsk intrusions, olivine-rich rocks are devoid of low-S minerals of the chalcopyrite group: Fe-rich chalcopyrite, putoranite, and talnakhite.

Major sulfide minerals are pyrrhotite and troilite (75–90 vol % of all sulfides). Rarely, their proportion decreases to 60% or increases up to 95%. The pyrrhotite is mainly represented by two morphological varieties. Pyrrhotite I composes large grains of irregular shape up to 4–10 mm in size, which contain lenticular and flame-like exsolutions of pentlandite II. Pyrrhotite II occurs as inclusions up to 0.1 mm in size with uneven or sharp straight edges, frequently of the similar orientation, in chalcopyrite. Pyrrhotite is frequently replaced by magnetite–marcasite–pyrite aggregate.

Pentlandite accounts for 3–8 vol % sulfides. It commonly occurs as thin (a few microns) lamellae, lenses, and flame-like exsolutions of pentlandite II, which are confined to the periphery of pyrrhotite grains and fractures in the latter. Scarcer pentlandite I forms small (<0.05 mm), irregularly shaped porphyritic phenocrysts and rims around pyrrhotite grains unless pentlandite rims are absent and pyrrhotite is resorbed by chalcopyrite.

In the lower parts of the ultramafic layer, the pyrrhotite group minerals are represented by hexagonal and monoclinic modifications, while pentlandite is represented by its Ni-rich variety (ESM_18.pdf (Suppl.)). The chemical composition of sulfides systematically varies depending on their association (ESM_18.pdf (Suppl.)). Hexagonal pyrrhotite contains 0.03–0.46 wt % Ni, troilite is essentially devoid of Ni, while monoclinic pyrrhotite contains up to 0.76 wt % Ni. Pentlandite in the association with troilite has the highest Fe content (32–39 wt % Fe), an intermediate composition (28–33 wt % Fe) in the association with hexagonal pyrrhotite, and is represented by the highest Ni variety (27–31 wt % Fe) in the association with monoclinic pyrrhotite. In the Zelenaya Griva intrusion, troilite associates with Fe-intermediate pentlandite (31–33 wt % Fe), while hexagonal pyrrhotite occurs with Ni-enriched pentlandite (ESM_18.pdf (Suppl.)). Pentlandites from the Lower Talnakh massifs have elevated Co content (2–10.6 wt %) both in the low-S and high-S associations.

Minerals of the chalcopyrite group (3–12 vol %, more rarely, up to 20 vol %) are represented by chalcopyrite, high-Fe chalcopyrite, more rarely putoranite and talnakhite. They form thin (<0.1 mm) discontinuous rims around sulfides, and more rarely occur between pyrrhotite grains and as lenses in pyrrhotite. Iron-rich chalcopyrite differs from common tetragonal chalcopyrite not only in the Fe/Cu ratio, but also in the elevated Ni concentration (ESM_18.pdf

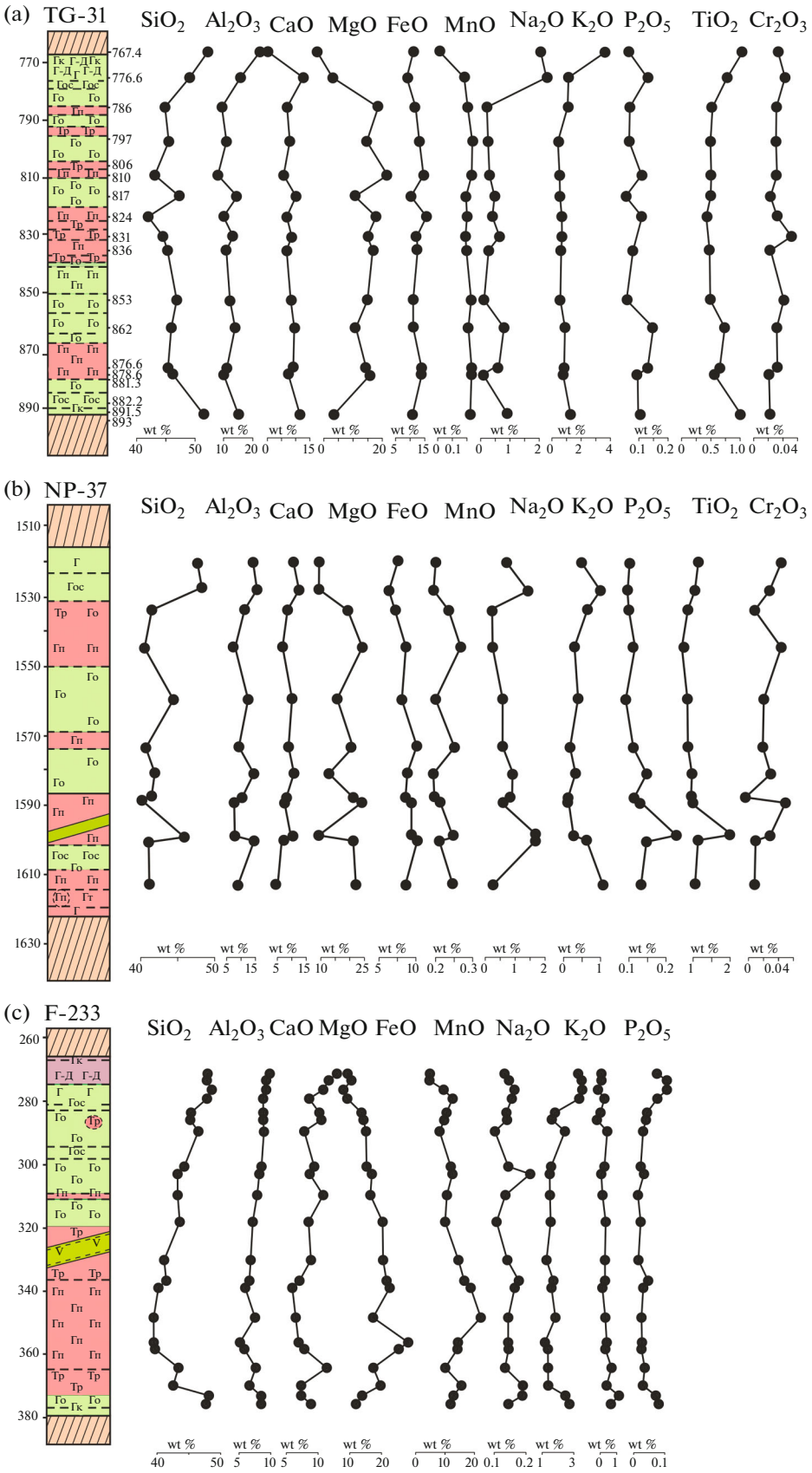

Fig. 10. Variations of oxide contents (wt %) in sections of the (a) Lower Talnakh (drill hole TG-31), (b) Lower Norilsk (drill hole NP-37), and (c) Zelenaya Griva (drill hole F-233) intrusions. For symbols, see Fig. 8.

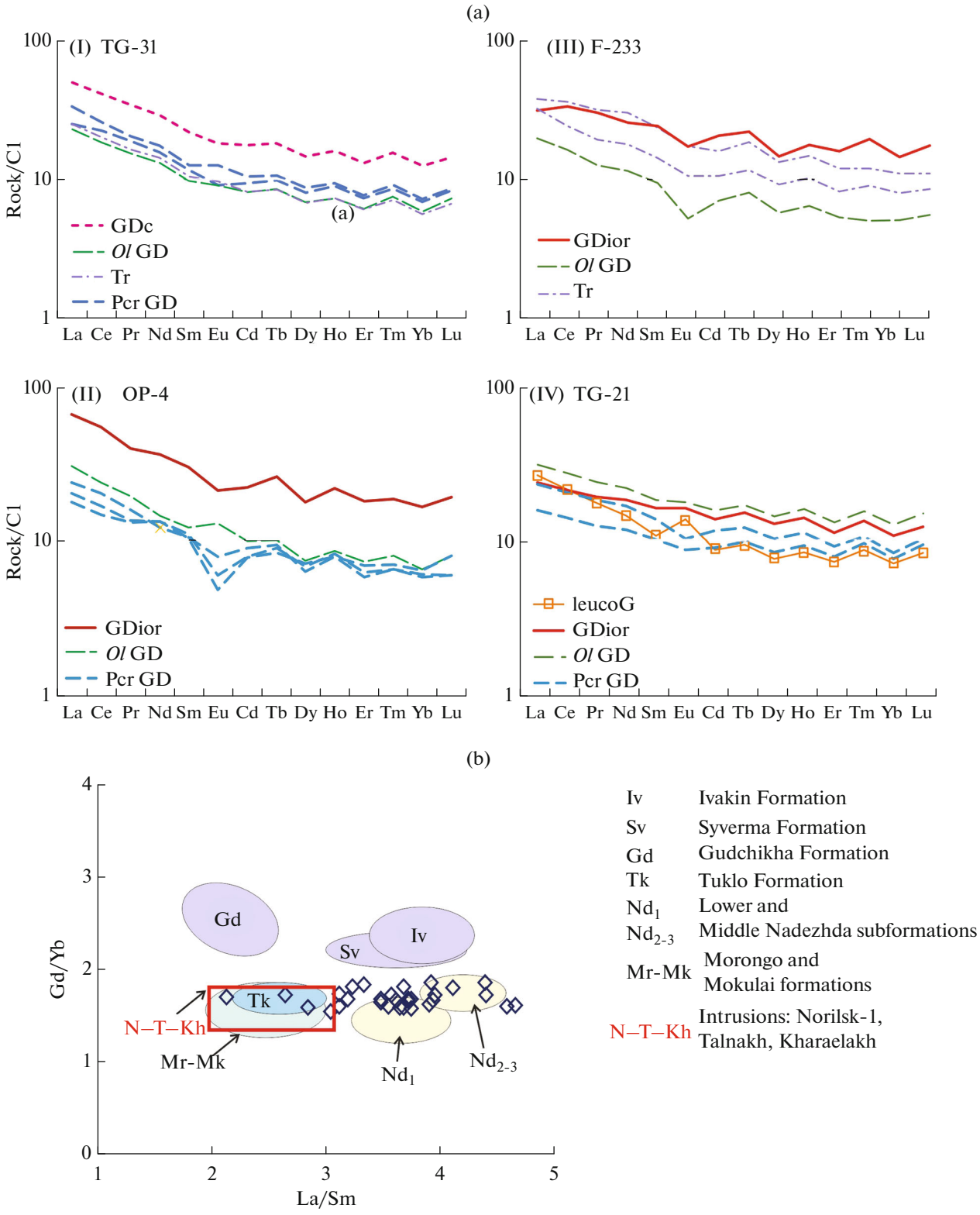

Fig. 11. Chondrite-normalized (McDonough and Sun, 1995) REE distribution patterns for rocks of the Lower Talnakh (drill hole TG-31 (1), drill hole OP-4 (2), Zelenaya Griva (drill hole F-233 (III)), and Kharaelakh (drill hole TG-21 (IV)) intrusions (a). (GDior) gabbrodiorite, (*Ol* GD) olivine gabbrodolerite, (Tr) troctolite, (Pcr GD) picritic gabbrodolerite, (GDc) contact gabbrodolerite, (leucoG) leucogabbro. (b) Diagram Gd/Yb–La/Sm for the rocks of the Lower Talnakh and Zelenaya Griva intrusions according to data on drill holes TG-31, OP-4, and F-233 (ESM_14 (Suppl.)) and drill hole SG-28 after (Czamanske et al., 1994). Compositional fields of volcanic formations are shown according to (Lightfoot et al., 1994; Naldrett et al., 1995).

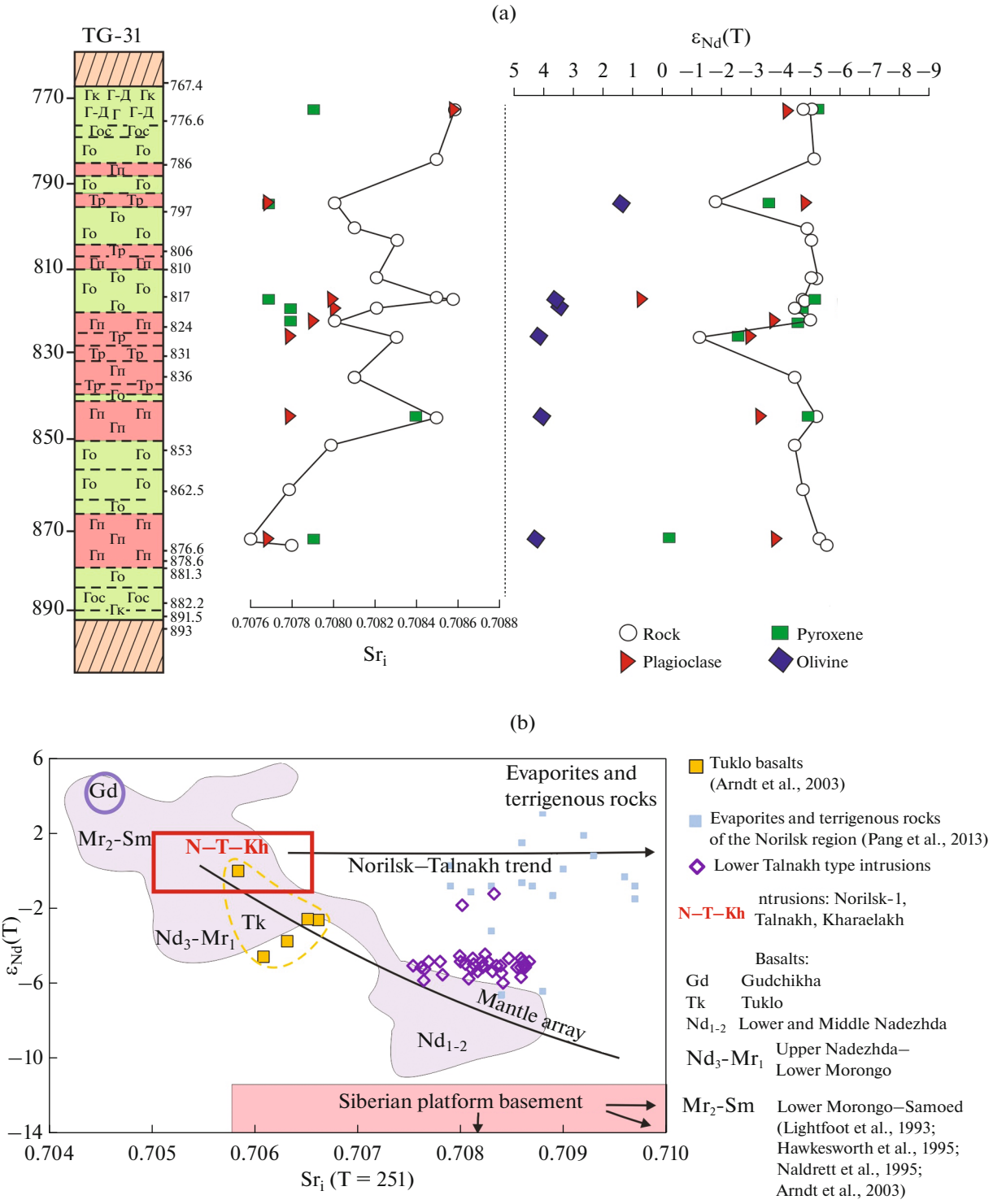

Fig. 12. Sr–Nd isotope systematics of rocks and minerals of the Lower Talnakh intrusion. (a) Variations of $Sr_i = {}^{87}Sr/{}^{86}Sr$ and $\varepsilon_{Nd}(T)$ (for an age of 250 Ma) in drill hole TG-31 section. For symbols, see Fig. 8; (b) isotope compositions of rocks of the Lower Talnakh intrusions in the Sr_i– $\varepsilon_{Nd}(T)$ diagram. Basement of the Siberian Platform is characterized based on the compositions of xenoliths in the Maslov pipe (Czamanske et al., 2000; Samsonov et al., 2022). Lines of the mantle mixing trend is shown in interpretation of (Arndt et al., 2003).

(Suppl.)). This mineral, along with putoranite, talnakhite, and mooihoekite, is affected by rapid oxidation being covered by the rusty-vary-colored film on air.

Cubanite (5–8 vol %) forms lamellae in minerals of the chalcopyrite group and granular aggregates. The granular cubanite has reaction relations with minerals of the pyrrhotite group, replacing the latter along the periphery of their aggregates and at the grain contacts.

Accessory minerals of the sulfide associations are represented by sphalerite, thiospinels, as well as Co, Ni and Fe arsenides and sulfoarsenides. The content of sphalerite (up to 2 vol %) exceeds its content in disseminated pyrrhotite ores of the economic ore-bearing intrusions. Pyrite together with chalcopyrite forms phenocrysts of an irregular shape in the upper and lower inner contact zones as well as in host rocks of the nearby exocontact.

Sulfur and Copper Isotope Composition

Most sulfides of the Lower Talnakh intrusions have $\delta^{34}S$ values ranging from 3.8 to 8.6‰, with both a mean and an average value of 5.7‰ (n = 28) (ESM_19.pdf (Suppl. 1)). However, in the upper and lower parts of the Zelenaya Griva intrusion, $\delta^{34}S$ values range from 9.2 to11.8‰, which is reflected in a higher mean $\delta^{34}S$ value of 9.3‰ (n = 10) for this intrusion (Fig. 13a).

The $\delta^{65}Cu$ values for sulfides of the Lower Talnakh intrusions vary from 0 to –1.1‰ (ESM_19.pdf (Suppl.)), with a mean of $\delta^{65}Cu = -0.6 \pm 0.4$‰ ($n$ = 15), which is close to those of ores of the Vologochan and Talnakh deposits (Fig. 13b).

Sulfide mineralization in the Lower Talnakh intrusions is characterized by the elevated Re content (119–316 ppm), low Os content (4.4–32.9 ppm), high Re/Os (13.7–71.6) and γOs (35.6–117.8) (Malitch et al., 2018), which are similar to the data by Arndt et al. (2003), which demonstrate the γOs variations within 10.2–71.

DISCUSSION

Crystallization Conditions of the Intrusions

The limited differentiated series at the absence of leucogabbro and magnetite gabbrodolerites, the absence of sharp boundaries between the different rock types, and the vague cryptic layering indicate a weak degree of in-stage differentiation of the Lower Talnakh type massifs. The taxitic varieties are saturated in plagioclase aggregates and clastic fragments of leucocratic gabbrodolerites that indicates the accumulation and floating of plagioclase cumulates occurring at a some depth in the intermediate chambers or along the transport pathways, whereas physical separation of plagioclase with its accumulation in the resident chamber is not expressed. A relatively homogenous chemical and petrographic composition of rocks shows that most the fragments are derivatives of the same magma. The non-cognate fragments, such as xenoliths of metasedimentary rocks widespread in taxitic and picritic rocks of the Norilsk type intrusions (Godlevsky, 1959: Turovtsev, 2002; Ryabov et al., 2014; Chayka et al., 2020), are much less abundant in Lower Talnakh rocks. They contain no fragments of chromite schlierens and trails of granulated olivine, which are the characteristic features of the Norilsk chonoliths being interpreted either as a result of brecciation or resorption of the earliest primitive cumulates (Zolotukhin, 1964) or as products of fluid recrystallization (Ryabov et al., 2014, P. 124).

Crystallization order in the olivine-bearing varieties, judging from the petrographic observations, corresponds to the universal scheme observed in all differentiated intrusions. The liquidus phase is olivine, while cotectic chrome spinel is very rare and significantly enriched in iron, which reflects both the primary low-Cr composition of the magma and postcumulus re-equilibration that led to the even greater depletion in Cr. As in the ore-bearing intrusions, clinopyroxene is crystallized later than olivine–plagioclase cotectic, as follows from the petrographic observations (Dyuzhikov et al., 1988; Ryabov et al., 2014) and modeling data (Krivolutskaya et al., 2001). The wide development of oikocrysts and interstitial grains of zoned clinopyroxene, which are typical of ore-bearing intrusions, is also observed in the Lower Talnakh type, but the elevated Cr content in the oikocryst core suggests the presence of clinopyroxene in liquidus association. Up to now, the origin of oikocrystic textures is a subject of debates, which overview is provided by Barnes et al. (2016). Alternative models consider their primary growth in situ as liquidus phase with long-term subsequent crystallization (Campbell, 1978; Barnes et al., 2016; Schoneveld et al., 2020), or later crystallization from intercumulus liquid as postcumulus phase. The presence of relatively high-Cr cores in clinopyroxene (up to 0.5 wt % Cr_2O_3) suggests its likely early crystallization in a ternary cotectic liquidus association with olivine and plagioclase likely in the staging chamber from yet high-Cr melt.

Orthopyroxene is present in the mineral associations as intercumulus and reaction phase, similar to its appearance in rocks of the ore-bearing intrusions. Its composition is in disequilibrium with the compositions of the cores and the rims of coexisting clinopyroxene and its presence is explained by the peritectic reaction of olivine with interstitial liquid showing prograde enrichment in silica.

Picritic and troctolite gabbrodolerites are olivine-rich cumulates introduced in chamber as magmatic suspension (slurry) with varying (albeit higher than in the ore-bearing intrusions) proportions of olivine and plagioclase antecrysts. The antecrysts are here referred to as early phenocrysts that crystallized in the mag-

matic plumbing system before the magma reached crystallization chamber and, therefore, likely experienced additional events (Jerram et al., 2018). This conclusion is consistent with the widespread cross-bedding and sorting of the grains, the narrow compositional variations in olivine, the prevalence of the high-Mg compositions $Fo_{75–83}$ (ESM_6.pdf (Suppl.)), the irregular occurrence of the picritic horizons at the different stratigraphic levels in the intrusion (Figs. 8, 9), and the medium- to fine-grained textures of inner contact rocks with the absence of chilled varieties that are typical of the Lower Talnakh type intrusions. During transportation and sorting of the magmatic slurry, an amount of melt increased at adiabatic decrease of melting temperature and partial dissolution of antecrysts that enriched this melt in Mg within the olivine-rich layers. This process determined the total high-Mg composition of the intrusion while allowing some degree of subsequent in-stage differentiation, which locally led to the formation of thick lenses of gabbrodiorites as crystallization products of a residual melt.

The similar crystallization sequence is observed in olivine porphyritic basalts, which are widespread in the volcanic formations of the Norilsk region from the Gudchikha to the Mokulai ones. Olivine in these rocks is the first liquidus phase, but glomerocrystic associations include both olivine, plagioclase and later clinopyroxene, which is characterized by the sharp Cr, Ti, and Mg# zoning. In addition, the differentiated picritic flows contain pyroxene porphyritic basalts, where clinopyroxene is a sole liquidus phase forming dendrites, spherulites, and porphyrocrysts (Ryabov et al., 2014). Olivine $Fo_{82–84}$ is known in the picritic basalts of the Gudchikha Formation, where it contains up to 0.4 wt % NiO (Krivolutskaya, 2014, Krivolutskaya et al., 2022; Ryabov et al., 2014) and is frequently surrounded by a rim of peritectic orthopyroxene, as well as found in picrites of the Tuklo Formation, where it is depleted in Ni (<0.2 wt % NiO after Ryabov et al., 2014). Younger tholeiitic basalts of the Nadezhda, Morongo, and Mokulai formations contain lower-Mg olivine (up to $Fo_{44–52}$ after Ryabov et al., 2014). The upper limit of of $Fo_{82–83}$ in picritic gabbrodolerites of the ore-bearing and Lower Talnakh intrusions thus coincides with those of picrites of the Gudchikha and Tuklo formations and suggests similar Mg# of their melts, given the close crystallization conditions and the composition of the liquidus association. According to the melt inclusion study, picritic melts that were in equilibrium with olivine of the Gudchikha Formation contained 48–49 wt % SiO_2 and 11–14 wt % MgO (Sobolev et al., 2009). It is known that olivine Mg# correlates with Mg# of parental melt with coefficient Kd(Fe–Mg) = 0.31–0.37, but has no direct correlation with MgO content in the melt (e.g., Matzen et al., 2011), which discards a direct analogy.

Rare-earth element systematics (Figs. 11a, 11b), which is used to discriminate the volcanic cycles in the Norilsk region (Lightfoot et al., 1990, 1993; Naldrett et al., 1995; Fedorenko, 2010; Krivolutskaya, 2014), shows that lavas of the first volcanic stage from the Ivakin to the Gudchikha formations have no geochemical affinity with the differentiated intrusions, which is consistent with the geological evidences of their asynchronous formation (Krivolutskaya, 2014; Rad'ko, 2016). In the La/Sm–Gd/Yb diagram (Fig. 11b), the compositional fields of the Lower Talnakh type intrusions are mainly overlapped with the compositions of the Nadezhda lavas, falling partly in the compositional fields of the younger volcanic rocks of the second stage and in the field of the ore-bearing intrusions.

Interpretation of Isotope-Geochemical Data

Generalizing available isotope-geochemical data (Fig. 11b), Fedorenko (2010) suggested that the derivatives of the Lower–Middle Nadezhda melts were derived from the Tuklo picritic magma through the removal of cumulates and assimilation in the intermediate chamber. This assumption is confirmed by modeling (Yao and Mungall, 2021), which showed that the Nadezhda melts could be derived through the evolution of the Tuklo magma with 25% contamination in the intermediate chamber by interaction with the Proterozoic basement characterized by the nonradiogenic Nd and highly radiogenic Sr isotope compositions (Fig. 12b). These researchers accepted the comagmatic origin of the Lower Talnakh intrusions and the Tuklo–Nadezhda magmas following (Naldrett et al., 1995; Arndt et al., 2003; Fedorenko, 2010), which is mainly based on their similar depletion in chalcophile elements. In the framework of this model (Yao and Mungall, 2021), Morongo–Mokulai tholeiitic basaltic melts were transported through intermediate chambers entrapping suspended crystals and sulfides, which have been precipitated from the Tuklo–Nadezhda magmas, to form the ore-bearing intrusions in the upper crust assimilating host sedimentary rocks. Such point of view is close to the model of melting and entrapment of ancient sulfide segregations by tholeiitic magmas (Krivolutskaya, 2014; Krivolutskaya et al., 2019) and does not support the existence of specific picritic ore-bearing magmas. At the same time, such multistage model allows the accumulation of sulfide ores from the great magma volume with ordinary primary contents of chalcophile elements and PGE. This model also includes the subsequent emplacement of intrusive bodies at the increasingly higher stratigraphic levels within an ore cluster (Yao and Mungall, 2021) that determines the Lower Talnakh type intrusions as the earliest ones.

The isotopic compositions of rocks of the Lower Talnakh type intrusions occupy a specific field in the diagram Sr_i–$\varepsilon_{Nd}(T)$ (Fig. 12b), which is generally

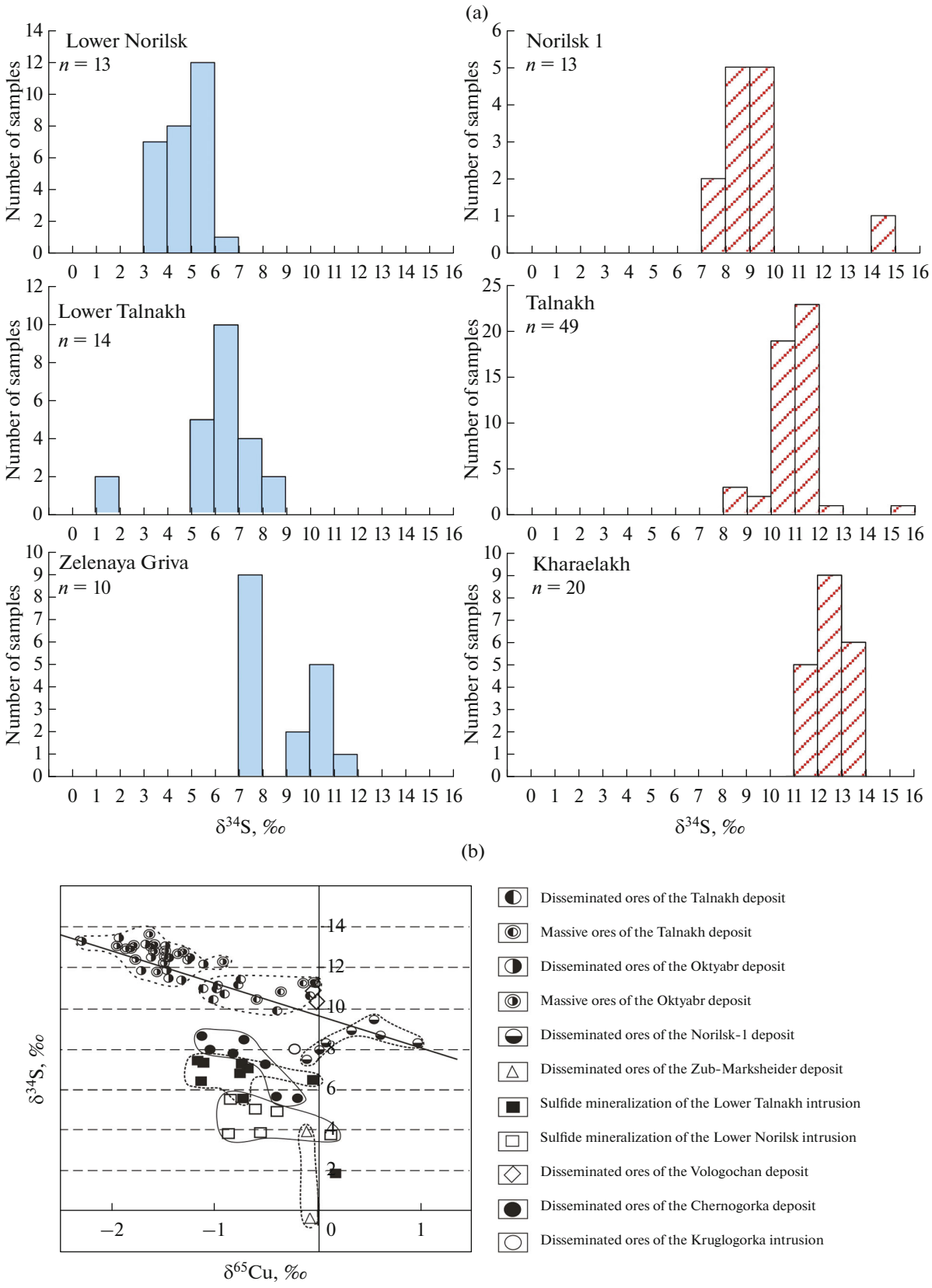

Fig. 13. Variations of S isotope composition of sulfide mineralization in the Lower Talnakh type intrusions in disseminated ores of the Norilsk type ore-bearing intrusions after Malitch et al. (2014) and according to the results of this study (a); (b) variations of S and Cu isotope composition of sulfide ores of the Norilsk intrusions in the $\delta^{65}Cu$–$\delta^{34}S$ diagram (Malitch et al., 2014; Sluzhenikin et al., 2018 and results of this study).

interpreted as a result of the assimilation of the Proterozoic basement in the mid-crustal chamber. The isotopic characteristics of the basement are obtained from analysis of the fragments of granitoid and metamorphosed sedimentary rocks, which were brought to the surface by the Maslov explosive pipe in the northern part of the Norilsk depression. The age of the fragments varies within 870–2600 Ma (Czamanske et al., 2000; Samsonov et al., 2022) and in general the isotope characteristics of the granitoids are extremely diverse ($\varepsilon_{Nd}(T)$ from –6 to –19 and Sr_i from 0.7057 to 0.7299). They plot in the right lower corner of the diagram and far beyond the scale shown in Fig. 12b. The Paleozoic sedimentary rocks sampled from drill hole sections in the Mikchangda and Kharaelakh depression (Pang et al., 2013) are also characterized by the widest variations ($\varepsilon_{Nd}(T)$ from –7 to +10 and Sr_i from 0.7079 to 0.7154). However, the majority of data points occupy the right upper corner of the diagram, and their compositional fields are not overlapped with the field of the Proterozoic basement (Fig. 12b). Therefore, the Sr-Nd isotope compositions of the Lower Talnakh type intrusions reveal the predominant contribution of Proterozoic material, unlike the ore-bearing intrusions, which Sr-Nd isotope systematics indicates the assimilation of the Paleozoic upper crustal material, forming so-called Norilsk–Talnakh trend according to the interpretation of previous researchers (Naldrett et al., 1995; Lightfoot et al., 1993; Arndt et al., 2003).

Our new data emphasize a subhorizontal trend of isotope variations in Lower Talnakh type rocks, which is approximately parallel to the Norilsk–Talnakh trend, but at lower values of $\varepsilon_{Nd}(T)$ from –4 to –6. Such trend could serve as a marker of the assimilation of sulfate-bearing Paleozoic material in the transport pathways and resident chamber that is well consistent with the elevated positive $\delta^{34}S$ up to 11.8‰ at the average values from 5.7 to 9.3‰ for the individual Lower Talnakh intrusions. The mineralized intrusions bear sulfide sulfur enriched in heavy isotope mainly within the range of 8–13‰ $\delta^{34}S$. Thereby, three intrusions with economic mineralization show an increase of average $\delta^{34}S$ from 8–9‰ in the Norilsk-1 to 10–11‰ in the Talnakh and ~12–13‰ in the Kharaelakh intrusion that correlated with increasing reserves of sulfide ores in this series (Grinenko, 1985; Malitch et al., 2014; *Izotopnaya geologiya* ..., 2017). This tendency was noted in the early studies by Grinenko (Grinenko, 1985) and confirmed by all subsequent investigatons, being one of the most important arguments in support of the assimilation of sulfate sulfur during formation of sulfide lodes.

The more detailed study of sulfides from the Lower Talnakh type intrusions revealed the greater heterogeneity of S isotope composition from 3.8 to 11.8‰. The heterogeneity of S isotope composition of sulfides is also observed within the ore-bearing intrusions, with progressive enrichment of the Kharaelakh intrusions in the isotopically heavy sulfur towards the front of the emplacement (Ketrov et al., 2022). At the low sulfide content, the low degree of their fractionation, and the extremely low tenor of base metals and PGE, the heterogeneous isotopically heavy S isotope composition of the Lower Talnakh type intrusions likely reflects the attainment of repeated local sulfide saturation owing to the assimilation of sedimentary sulfate S. Sulfur was extracted during crystallization of the magmatic suspension, which has been exhausted in chalcophile metals due to their earlier losses into coexisting sulfide liquid at a depth.

The crustal nature of sulfide S in the Lower Talnakh type intrusions is consistent with the high γOs values (Arndt et al., 2003; *Izotopnaya geologiya* ..., 2017; Malitch et al., 2018), which also support the loss of Os into coexisting sulfides at a depth. For this reason, the relatively low degree of contamination in the resident chamber significantly modified the Re-Os isotope characteristics of few Os-depleted sulfides.

The Cu isotope composition of the Lower Talnakh type intrusions overlaps with those compositions of the Talnakh and Chernogorka ore-bearing intrusions. In the $\delta^{65}Cu$–$\delta^{34}S$ diagram, the compositions of the Lower Talnakh type sulfides plot far away from a trend of negative correlation defined for three economic ore-bearing intrusions (Malitch et al., 2014). The affiliation to this trend is considered as an indicator of ore potential (Malitch et al., 2018), although process controlling this distribution is unclear yet.

Relations of the Lower Talnakh and Ore-Bearing Norilsk-Type Intrusions

In the Talnakh ore cluster, the Lower Talnakh type intrusions are located stratigraphically lower than the ore-bearing and Kruglogorka type intrusions (Fig. 4, ESM_3.pdf–ESM_4.pdf (Suppl.)), however, in the northern areas, the Talnakh intrusion lies below the Lower Talnakh intrusion. In some areas, these intrusions are in contact (ESM_4.pdf (Suppl.)), but chilled zones are not observed. The later emplacement of the Talnakh intrusion is believed to be supported by the presence of sulfide mineralization in the upper inner contact of the Lower Talnakh intrusion, where it is located beneath the ore-bearing intrusion (Avgustinchik, 1981). This mineralization is interpreted as superimposed on rocks of the upper inner contact of the Lower Talnakh massif. According to our concept, the mineralization in the upper inner contact is typical of some massifs and is, likely, unrelated to the later injections of ore-bearing magmas. In addition, there are evidence of injections of the Lower Talnakh intrusion into the ore-bearing Talnakh intrusion (Sukhareva and Kuznetsova, 1983) that suggests simultaneous or later emplacement of the Lower Talnakh intrusion.

The distribution of thicknesses in the Western branch of the Lower Talnakh massif is interpreted as controlling the distribution of the apophyses of the Kharaelakh intrusion, assuming that the emplacement of the branches of the Lower Talnakh intrusion provided a favorable setting for the emplacement of subsequent intrusions. Thereby, the graben-like reverse faults, which complicate the periphery of the depression, have been used as the pathways and reworked by the intrusions. However, an alternative interpretation can be proposed: the emplacement of the ore-bearing chonolith created a space for the emplacement of the Lower Talnakh type magmas and cumulates. Most researchers accepted that the Kruglogorka sills are older than the ore-bearing chonoliths (Rad'ko, 2016; Sluzhenikin et al., 2015; Likhachev, 1994, 2006). However, the question of time constraints for the emplacement of the Lower Talnakh magmas is still far from solution, because none of these hypotheses provided convincing evidences. Some authors (Dyuzhikov et al., 1988; Ryabov et al., 2014) suggested the latest emplacement of the Lower Talnakh intrusions, but noted that the order of the emplacement cannot be considered to be unambiguous for all the ore clusters.

In any case, important prospecting significance of the Lower Talnakh intrusions is based on their structural-spatial association with the ore-bearing chonoliths in the Talnakh, Norilsk, and Talmi ore cluster. In the last cluster located at the margin of the Yenisei–Khatanga trough and confined to the Norilsk–Kharaelakh fault zone in the north of the Kharaelakh depression, the Talmi fully differentiated intrusion associates with the Lower Talnakh type Klyukvenny melanocratic intrusion (Dyuzhikov et al., 1988).

Based on the general geological considerations, the weakly differentiated Lower Talnakh melanocratic intrusions, the Kruglogorka leucocratic intrusions and the differentiated intrusions of mesocratic type were likely formed from separate deep portions of primary picritic magma with different history of stagnation, contamination, and crustal differentiation. The Kruglogorka leucocratic intrusions are characterized by the elevated thickness of leucogabbros resulted from the flotation of plagioclase cumulate, but do not contain the corresponding amount of picritic rocks and sulfide ores, although show no depletion in chalcophile elements. In contrast, the melanocratic intrusions are made up of olivine cumulates depleted in chalcophile metals, in the absence of corresponding fraction of plagioclase cumulates. Accepting that the ore-bearing mesocratic intrusions are made up of a full differentiated series corresponding to the evolution of parental picritic melt, it can be suggested that the incomplete series are formed by magma layering in the intermediate zones of crustal partial melting, which structure is similar to the observed upper crustal multi-floor intrusive buildups. The isotope-geochemical data indicate the longer residence time of the Lower Talnakh type magmas at the deeper crustal levels, which is consistent with the hypothesis of their later emplacement. The ultramafic composition of their sequences is related to the transportation of olivine cumulates as crystal slurry (suspension) assuming that significant part of the most primitive olivine–chromite cumulates has remained at a depth. Adiabatic decompressional melting and resorption of cumulates during transportation into the low pressure zones increased the melt fraction, which provided conditions for differentiation in the modern chamber. The long-term stagnation in the crust resulted in the crustal characteristics of the magmas, their exhaustion in the ore elements (Ni, Cu, Cr, and PGE) in favor of coexisting cumulates (oxide–silicate and sulfide) and migrating ore-bearing melts. Thus, our hypothesis suggests that the melanocratic intrusions were formed in the Morongo–Mukulai time, as was substantiated in (Rad'ko, 2016), at the second volcanic stage. In compliance with the earlier interpretations (Dyuzhikov et al., 1988; Ryabov et al., 2014), the Kruglogorka type intrusions have been emplaced first, followed by the ore-bearing Norilsk type and then by the Lower Talnakh type intrusions. According to this hypothesis, all differentiated intrusions of the Norilsk complex are derivatives of a primary picritic melt, but none of their parental magmas represented the primary mantle-derived melt. The distinctions in the differentiated series and ore potential are related to the contrasting parameters of crustal contamination such as the composition of contaminant, duration and scale of interaction with it, history of hybridization or mixing with other liquids, the timing of sulfide and fluid immiscibility, the degree of fractional crystallization of partial melts in the intermediate layered storage zone, and *P-T* conditions in it.

ACKNOWLEDGMENTS

We are grateful for fruitful discussion to our colleagues from research and prospecting organizations, especially to geologists of the Norilskgeologii (NNTS Technical Services), whose efforts significantly clarified the geological structure of the Norilsk ore region. We are grateful to V.S. Kamenetsky and I.F. Chayka for critical comments and suggestions, which helped us to specify obtained data.

FUNDING

The studies were supported by the Russian Science Foundation (project no. 21–17–00119/https://rscf.ru/project/21–17–00119) with partial support of isotope studies by government-financed task no. 122022600107–1 of the Institute of Geology and Geochemistry of the Ural Branch of the Russian Academy of Sciences.

CONFLICT OF INTEREST

The authors declare that they have no conflicts of interest.

SUPPLEMENTARY INFORMATION

The online version contains supplementary material available at https://doi.org/10.1134/S0869591123050065.

REFERENCES

Arndt, N.T., Czamanske, G.K., and Walker, R.J., Geochemistry and origin of the intrusive hosts of the Noril'sk–Talnakh Cu–Ni–PGE sulfide deposits, *Econ. Geol.,* 2003, vol. 98, pp. 495–515.

Avgustinchik, I.A., On the composition of sulfide mineralization in the Lower Talnakh intrusion, *Genezis i usloviya lokalizatsii medno-nikelevogo orudeneniya* (Genesis and Localization Conditions of the Copper–Nickel Mineralization), Moscow: TsNIGRI, 1981, pp. 34–40.

Barnes, S.J. and Mole, D.R., Le Vaillant, M., et al., Poikilitic textures, heteradcumulates and zoned orthopyroxenes in the Ntaka ultramafic complex, Tanzania: implications for crystallization mechanisms of oikocrysts, *J. Petrol.,* 2016, vol. 57, no. 6, pp. 1171–1198.

Bychkova, Ya.V., Sinitsyn, M.Yu., and Petrenko, D.B., Method peculiarities of multielemental analysis of rocks with inductively-coupled plasma mass spectrometry, *Moscow Univ. Geol. Bull.,* 2016, vol. 72, no. 1, pp. 56–62.

Godlevskii, M.N., *Trappy i rudonosnye intruzii Noril'skogo raiona* (Traps and Ore-Bearing Intrusions of the Norilsk Region), Moscow: Gosgeoltekhizdat, 1959.

Campbell, I.H., Some problems with the cumulus theory, *Lithos,* 1978, vol. 11, pp. 311–323.

Chayka, I.F., Kamenetsky, V.S., Zhitova, L.M., et al., Hybrid nature of the platinum group element chromite-rich rocks of the Norilsk-1 intrusion: genetic constraints from Cr spinel and spinel-hosted multiphase inclusions, *Econ. Geol.,* 2020, vol. 115, pp. 1321–1342.

Czamanske, G.K., Kunilov, V.E., Zientek, H.L., et al., A proton-microprobe study of magmatic sulfi de ores from the Noril'sk–Talnakh district, Siberia, *Can. Mineral.,* 1992, vol. 30, pp. 249–287.

Czamanske, G.K., Wooden, J.L., Zientek, H.L., et al., Geochemical and isotopic constrains of the petrogenesis of the Noril'sk–Talnakh ore-forming systems, *Sudbury-Noril'sk Symposium, Ontario Geol. Surv. Spec.,* 1994, vol. 5, pp. 313–341.

Czamanske, G.K., Wooden, J.L., Walker, R.J., et al., Geochemical, isotopic, and SHRIMP age data for Precambrian basement rocks, Permian volcanic rocks, and sedimentary host rocks to the ore-bearing intrusions, Noril'sk–Talnakh district, Siberian Russia, *Int. Geol. Rev.,* 2000, vol. 42, no. 10, pp. 895–927.

Dodin, D.A. and Sadikov, M.A., Some questions of differentiated traps by the example of the Kharaelakh Mountains, *Petrologiya trappov Sibirskoi platform* (Petrology of Traps of the Siberian Platform), Leningrad: Nedra, 1967, pp. 141–152.

Dyuzhikov, O.A., Distler, V.V., Strunin, B.M., et al., *Geologiya i rudonosnost' Noril'skogo raiona* (Geology and Ore Potential of the Norilsk Region), Moscow: Nedra, 1988.

Fedorenko, V.A., *Magmatizm i medno-nikelevye mestorozhdeniya Noril'skogo raiona* (Magmatism and Copper–Nickel Deposits of the Norilsk Region), Noril'sk: Fondy Noril'skgeologii, 2010.

Grinenko, L.N., Sources of sulfur of the nickeliferous and barren gabbro-dolerite intrusions of the northwest Siberian Platform, *Int. Geol. Rev.,* 1985, vol. 28, pp. 695–708.

Hawkesworth, C.J., Lightfoot, P.C., Fedorenko, V.A., et al., Magma differentiation and mineralisation in the Siberian flood basalts, *Lithos,* 1995, vol. 34, pp. 61–88.

Izotopnaya geologiya noril'skikh mestorozhdenii (Isotope Geology of the Norilsk Deposits), Petrov, O.V, Eds., St. Petersburg: VSEGEI, 2017.

Jerram, D.A., Dobson, K.J., Morgan, D.J., and Pankhurs, M.J., *The petrogenesis of magmatic systems: using igneous textures to understand magmatic processes, Volcanic and Igneous Plumbing Systems,* Burchardt, S., Eds., Amsterdam: Elsevier, 2018, pp. 191–229.

Ketrov, A.A., Yudovskaya, M.A., Shelukhina, Yu.S., et al., Sources and evolution of sulfur isotopic composition of sulfides of the Kharaelakh amd Pyasino–Vologochan intrusions, Norilsk ore region, *Geol. Ore Deposits,* 2022, vol. 64, no. 6, pp. 350–376.

Komarova, M.Z. and Lyul'ko, T.P., On subdivision of trap intrusions of the Norilsk region, *Petrologiya trappov Sibirskoi platform* (Petrology of Traps of the Siberian Platform), Leningrad: Nedra, 1967, pp. 43–54.

Krivolutskaya, N.A., *Evolyutsiya trappovogo magmatizma i Pt-Cu-Ni rudoobrazovanie v Noril'skom raione* (Evolution of Trap Magmatism and Pt–Cu–Ni Ore Formation in the Norilsk Region), Moscow: Tovarishchestvo nauchnykh izdanii KMK, 2014.

Krivolutskaya, N.A., Ariskin, A.A., Sluzhenikin, S.F., and Turovtsev, D.M., Geochemical thermometry of rocks of the Talnakh Intrusion: assessment of the melt composition and the crystallinity of the parental magma, *Petrology,* 2001, vol. 9, no. 5, pp. 389–414.

Krivolutskaya, N.A., Latyshev, A.V., Dolgal, A.S., et al., Unique PGE–Cu–Ni Norilsk deposits, siberian trap province: magmatic and tectonic factors in their origin, *Minerals,* 2019, vol. 9, no. 1, Art. 66.

Krivolutskaya, N., Mikhailov, V., Gongalsky, B., et al., The Permian-Triassic riftogen rocks in the Norilsk area (NW Siberian Province): geochemistry and their possible link with PGE–Cu–Ni mineralization, *Minerals,* 2022, vol. 12, p. 1203.

Larson, P.B., Maher, K., Ramos, F.C., et al., Copper isotope ratios in magmatic and hydrothermal ore-forming environments, *Chem. Geol.,* 2003, vol. 201, nos. 3–4, pp. 337–350.

Lightfoot, P.C., Naldrett, A.J., Gorbachev, N.S., et al., Geochemistry of the Siberian trap of the Noril'sk area, USSR, with implication for the relative contributions of crust and mantle to flood basalt magmatism, *Contrib. Mineral. Petrol.,* 1990, vol. 104, pp. 631–644.

Lightfoot, P.C., Hawkesworth, C.J., Hergt, J., et al., Remobilisation of the continental lithosphere by mantle plumes: major-, trace-element, and Sr-, Nd-, and Pb-isotope evidence from picritic and tholeiitic lavas of the Norilsk District, Siberian Trap, Russia, *Contrib. Mineral. Petrol.,* 1993, vol. 114, pp. 171–188.

Lightfoot, P.C., Naldrett, A.J., Gorbachev, N.S., et al., Chemostratigraphy of Siberian trap lavas, Noril'sk District: implications for the source of floodbasalt 1378 magmas and their associated Ni–Cu mineralization, *Proc. Sudbury–No-*

ril'sk Symposium. Ontario Geol. Surv. Spec., 1994, vol. 5, pp. 283–312.

Likhachev, A.P., *Platino-medno-nikelevye i platinovye mestorozhdeniya* (Platinum–Copper–Nickel and Platinum Deposits), Moscow: Eslan, 2006.

Likhachev, A.P., Ore-bearing intrusions of the Noril'sk region, *Proc. Sudbury–Noril'sk Symposium. Ontario Geol. Surv. Spec.,* 1994, vol. 5, pp. 185–201.

Lyul'ko, V.A., Amosov, Yu.N., and Lunin, E.B., *Metallogenicheskaya karta (na med' i nikel') Severozapadnoi chasti Sibirskoi platformy masshtaba 1 : 200000* (Metallogenic Map (for Copper and Nickel). Northwestern Siberian Platform on a Scale 1 : 200000), Noril'sk: NKGRE, Fondy Noril'skgeologii, 1975.

Le Maitre, R.W., *Igneous Rocks. A Classification and Glossary of Terms. Recommendations of the International Union of Geological Sciences Subcommission on the Systematics of Igneous Rocks,* Cambridge: Cambridge University Press, 2002.

Malitch, K.N., Badanina, I.Yu., Belousova, E.A., et al., Contrasting magmatic sources in the ultramafic intrusions of the Norilsk region (Russia): Hf isotope data in zircon, *Ul'trabazit-bazitovye kompleksy skladchatykh oblastei i svyazannye s nimi mestorozhdeniya. Materialy III Mezhdunarodnoi konferentsii* (Ultramafic–Mafic Complex of Orogenic Areas and Related Deposits. Proc. 3rd International Conference), Yekaterinburg: IGG UrO RAN, 2009, vol. 2, pp. 35–38.

Malitch, K.N., Latypov, R.M., Badanina, I.Yu., and Sluzhenikin, S.F., Insights into ore genesis of Ni–Cu–PGE sulfide deposits of the Noril'sk province (Russia): evidence from copper and sulfur isotopes, *Lithos,* 2014, vol. 204, pp. 172–187.

Malitch, K.N., Badanina, I.Yu., Tuganova, E.V., *Rudonosnye ul'tramafit-mafitovye intruzivy Polyarnoi Sibiri: vozrast, usloviya obrazovaniya, kriterii prognoza* (Ore-Bearing Ultramafic–Mafic Intrusions of the Polar Siberia: Age, Conditions of Formation, and Prediction Criteria) Ekaterinburg: IGG UrO RAN, 2018.

Malitch, K.N., Belousova, E.A., Griffin, W.L., et al., New insights on the origin of ultramafic-mafic intrusions and associated Ni–Cu–PGE sulfide deposits of the Noril'sk and Taimyr provinces, Russia: evidence from radiogenic- and stable-isotope data, *Processes and Ore Deposits of Ultramafic-Mafic Magmas Through Space and Time* Mondal, S., Griffin, W.L., (Elsevier Inc, 2018), pp. 197–238.
https://doi.org/10.1016/0012-821X(76)90219-3

Matzen, A.K., Baker, M.B., Beckett, J.R., and Stolper, E.M., Fe–Mg partitioning between olivine and high-magnesian melts and the nature of Hawaiian parental liquids, *J. Petrol.,* 2011, vol. 52, pp. 1243–1263.

McDonough, W.F. and Sun, S.-S., The composition of the Earth, *Chem. Geol.,* 1995, vol. 120, pp. 223–253.

Naldrett, A.J., Lightfoot, P.C., Fedorenko, V.A., et al., Geology and geochemistry of intrusions and flood basalts of the Noril'sk region, USSR, with implication to the origin of the Ni–Cu ores, *Econ. Geol.,* 1992, vol. 87, pp. 975–1004.

Naldrett, A.J., Fedorenko, V.A., Lightfoot, P.C., et al., Ni–Cu–PGE deposits of Noril'sk region, Siberia: their formation in conduits for flood basalt volcanism, *Trans. Inst. Min. Metall., Sect. B,* 1995, vol. 104, pp. B18–B36.

Natorkhin, I.A., Arkhipova, A.I., and Batuev, B.N., *Petrologiya talnakhskikh intruzii* (Petrology of eh Talnakh Intrusions) Leningrad: Nedra, 1977.

Okuneva, T.G., Karpova, S.V., Streletskaya, M.V., et al., The method for Cu and Zn isotope ratio determination by MC-ICP-MS using the AG-MP-1 resin, *Geodynam. Tectonophys.,* 2022, vol. 13, no. 2s, 0615.
https://doi.org/10.5800/GT-2022-13-2s-0615

Paderin, P.G., Demenyuk, A.F., Nazarov, D.V., et al., *Gosudarstvennaya geologicheskaya karta Rossiiskoi Federatsii. Masshtab 1 : 1000000 (tret'e pokolenie). Seriya Noril'skaya. List R-45. Ob"yasnitel'naya zapiska* (State Geological Map of the Russian Federation. Scale 1 : 1000000 (Third Generation). Norilsk Series. Sheet R-45. Explanatory Note), St. Petersburg: Kartograficheskaya fabrika VSEGEI, 2016.

Pang, K-N., Arndt, N., Svensen, H., et al., A petrologic, geochemical and Sr-Nd isotopic study on contact metamorphism and degassing of Devonian evaporites in the Norilsk aureoles, Siberia, *Contrib. Mineral. Petrol.,* 2013, vol. 165, pp. 683–704.

Pin, C., Joannon, S., and Bosq, Ch., Le fevre B., Gauthier P.J. precise determination of Rb, Sr, Ba, and Pb in geological materials by isotope dilution and ICP-quadrupole mass spectrometry following separation of the analytes, *J. Analyt. Atom. Spectrom.,* 2003, vol. 18, pp. 135–141.

Putirka, K.D., Thermometers and barometers for volcanic systems, *Rev. Mineral. Geochem.,* 2008, vol. 69, pp. 61–120.

Rad'ko, V.A., *Fatsii intruzivnogo i effuzivnogo magmatizma Noril'skogo raiona* (Facies of the Intrusive and Effusive Magmatism of the Norilsk Region), St. Petersburg: Kartograficheskaya fabrika VSEGEI, 2016.

Richard, P., Shimizu, N., and Allegre, C.J., $^{143}Nd/^{144}Nd$ a natural tracer: an application to oceanic basalts, *Earth Planet. Sci. Lett.,* 1976, vol. 31.
https://doi.org/10.1016/0012-821X(76)90219-3

Ryabov, V.V., Shevko, A.Ya., and Gora, M.P., *Magmaticheskie porody Noril'skogo raiona. T. 1. Petrologiya trappov* (Magmatic Rocks of the Norilsk Region. Volume 1. Trap Petrology), Novosibirsk: Nonparel', 2000.

Ryabov, V.V., Shevko, A.Y., and Gora, M.P., *Trap Magmatism and Ore Formation in the Siberian Noril'sk Region* (Springer, 2014).

Samsonov, A.V., Sluzhenikin, S.F., Larionova, Yu.O., et al., 870-Ma active margin in the northwestern corner of the Siberian Craton: data on xenoliths from Late Permian explosibe Maslovskaya diatreme, Norilsk region, *Tektonika i geodinamika Zemnoi kory i mantii: fundamental'nye problemy. Materialy LIII Tektonicheskogo soveshchaniya* (Tectonics and Geodynamics of the Earths' Crust and Mantle: Fundamental Problems. Proc. 54th Tectonic Conference), Moscow: GEOS, 2022, vol. 2, pp. 168–172.

Schoneveld, L., Barnes, S.J., Godel, B., et al., Oxide–sulfide–melt–bubble interactions in spinel-rich taxitic rocks of the Norilsk–talnakh intrusions, Polar Siberia, *Econ. Geol.,* 2020, vol. 115, pp. 1305–1320.

Sluzhenikin, S.F. and Krivolutskaya, N.A., Pyasino–Vologochan intrusion: geological structure and platinum–copper–nickel ores (Norilsk Region), *Geol. Ore Deposits,* 2015, vol. 57, no. 5, pp. 381–401.

Sluzhenikin, S.F., Malitch, K.N., and Grigor'eva, A.V., "Differentiated mafic–ultramafic intrusions of the Kru-

glogorsky Type in the Noril'sk area: petrology and ore potential, *Petrology,* 2018, vol. 26, no. 3, pp. 280–313.

Sluzhenikin, S.F., Malitch, K.N., Turovtsev, D.M., et al., Differentiated mafic–ultramafic intrusions of the Zubovsky Type in the Norilsk Area: petrochemistry, geochemistry, and ore potential, *Petrology,* 2020, vol. 28, no. 5, pp. 458–490.

Sluzhenikin, S.F., Yudovskaya, M.A., Barnes, S.J., et al., Low-sulfide platinum group element ores of the norilsk-talnakh camp, *Econ. Geol.,* 2020, vol. 115, pp. 1267–1303.

Sobolev, A.V., Krivolutskaya, N.A., and Kuzmin, D.V., Petrology of the parental melts and mantle sources of Siberian trap magmatism, *Petrology*, 2009, vol. 17, no. 3, pp. 253–286.

Sukhareva, M.S. and Kuznetsova, N.P., On question of relations of differentiated intrusions of the Talnakh ore cluster: evidence from northern flanks, *Trappovyi magmatizm Sibirskoi platformy v svyazi s tektonikoi i poiskami poleznykh iskopaemykh. Tez. dokl.* (Trap Magmagism of the Siberian Platform in Relation with Tectonics and Prospecting of Mineral Resources. Abstracts), Krasnoyarsk: Krasnoyarsk-geologiya, 1983, pp. 89–92.

Turovtsev, D.M., *Kontaktovyi metamorfizm noril'skikh intruzii* (Contact Metamorphism of the Norilsk Intrusions), Moscow: Nauchnyi mir, 2002.

Yao, Z. and Mungall, J.E., Linking the Siberian flood basalts and giant Ni–Cu–PGE sulfide deposits at Norilsk, *J. Geophys. Res. Solid. Earth*, 2021.
https://doi.org/10.1029/2020JB020823

Zemskova, G.V., Petrographic characteristics of the Lower Talnakh type intrusions (Norilsk region), *Genezis i usloviya lokalizatsii medno-nikelevogo orudeneniya* (Genesis and Conditions of Localization of the Copper–Nickel Mineralization), Moscow: TsNIGRI, 1981, pp. 28–34.

Zen'ko, T.E. and Czamanske, G.K., Spatial and petrologic aspects of the intrusions of the Noril'sk–Talnakh ore junctions, Siberia, *Ontario Geol. Surv. Spec.,* 1994, vol. 5, pp. 263–282.

Zolotukhin, V.V., *Osnovnye zakonomernosti prototektoniki i voprosy formirovaniya rudonosnykh trappovykh intruzii (na primere Noril'skoi)* (Main Tendencies of Prototectonics and Questions of Formation of Ore-Bearing Trap Intrusions with Reference to the Norilsk Intrusion), Moscow: Nauka, 1964.

Translated by M. Bogina